

**DESIGN AND CONSTRUCTION OF A RESPIRATORY MOTION  
PHANTOM FOR TESTING THE TARGETING ACCURACY OF  
THE CYBERKNIFE SYSTEM WITH THE SYNCHRONY<sup>®</sup>  
RESPIRATORY TRACKING SYSTEM**

**CHIRASAK KHAMFONGKHRUEA**

**A THESIS SUBMITTED IN PARTIAL FULFILLMENT  
OF THE REQUIREMENTS FOR THE DEGREE OF  
MASTER OF SCIENCE (MEDICAL PHYSICS)  
FACULTY OF GRADUATE STUDIES  
MAHIDOL UNIVERSITY  
2010**

**COPYRIGHT OF MAHIDOL UNIVERSITY**

Thesis  
entitled

**DESIGN AND CONSTRUCTION OF A RESPIRATORY MOTION  
PHANTOM FOR TESTING THE TARGETING ACCURACY OF  
THE CYBERKNIFE SYSTEM WITH THE SYNCHRONY®  
RESPIRATORY TRACKING SYSTEM**

.....  
Mr. Chirasak Khamfongkhrua  
Candidate

.....  
Lect. Puangpen Tangboonduangjit, Ph.D.  
Major advisor

.....  
Lect. Pornpan Yongvithisatid, M.Sc.  
Co-advisor

.....  
Asst. Prof. Chirapha Tannanonta, M.Sc.  
Co-advisor

.....  
Asst. Prof. Auemphorn Mutchimwong,  
Ph.D.  
Acting Dean  
Faculty of Graduate Studies  
Mahidol University

.....  
Lect. Puangpen Tangboonduangjit, Ph.D.  
Program Director  
Master of Science Program in  
Medical Physics  
Faculty of Medicine Ramathibodi  
Hospital, Mahidol University

Thesis  
entitled  
**DESIGN AND CONSTRUCTION OF A RESPIRATORY MOTION  
PHANTOM FOR TESTING THE TARGETING ACCURACY OF  
THE CYBERKNIFE SYSTEM WITH THE SYNCHRONY®  
RESPIRATORY TRACKING SYSTEM**

was submitted to the Faculty of Graduate Studies, Mahidol University  
for the degree of Master of Science (Medical Physics)

on  
May 25, 2010

.....  
Mr. Chirasak Khamfongkhrua  
Candidate

.....  
Assoc. Prof. Sivalee Suriyapee, M.Eng.  
Chair

.....  
Lect. Puangpen Tangboonduangjit, Ph.D.  
Member

.....  
Asst. Prof. Chirapha Tannanonta, M.Sc.  
Member

.....  
Lect. Pornpan Yongvithisatid, M.Sc.  
Member

.....  
Asst. Prof. Auemphorn Mutchimwong,  
Ph.D.  
Acting Dean  
Faculty of Graduate Studies  
Mahidol University

.....  
Prof. Rajata Rajatanavin, M.D., F.A.C.E.  
Dean  
Faculty of Medicine Ramathibodi  
Hospital, Mahidol University

## ACKNOWLEDGEMENTS

The success of this thesis can be succeeded by the attentive support from my major advisor, Dr. Puangpen Tangboonduangjit and my co-advisor, Lect. Pornpan Yongvithisatid and Assist. Prof. Chirapha Tannanonta. I deeply thank them for their valuable advice, kind suggestion and guidance in my thesis.

I would like to thank, Assoc. Prof. Dr. Vipa Boonkiticharoen, program director of medical physics, faculty of medicine, Ramathibodi Hospital for valuable advice and comment in the research proposal.

I would like to thank, Lect.Somnuek Montonchunlaked at the Department of Radiology, Faculty of Medicine, Ramathibodi Hospital for his suggestion and assistance in design and construction of the respiratory motion phantom used in my research.

I would like to thank, Miss Kumutinee Pairat, Miss Patchareporn Dechsupa and Mr.Thawisak U-Khamphan in Radiosurgery Department, Faculty of Medicine, Ramathibodi Hospital for their help in my thesis experiment, being nice and friendly.

I would like to thank, my friends, Medical Physics Students in Medical Physics School, Faculty of Medicine, Ramathibodi Hospital for friendship and their help in studying in this course.

I am grateful to all the lecturers and Medical Physics staff, Faculty of Medicine, Ramathibodi Hospital for teaching me in medical physics knowledge.

Finally, I am grateful to my family for their financial support, entirely care, and love.

Chirasak Khamfongkhrua

**DESIGN AND CONSTRUCTION OF A RESPIRATORY MOTION PHANTOM FOR TESTING THE TARGETING ACCURACY OF THE CYBERKNIFE SYSTEM WITH THE SYNCHRONY<sup>®</sup> RESPIRATORY TRACKING SYSTEM****CHIRASAK KHAMFONGKHRUEA 5036373 RAMP/M****M.Sc. (MEDICAL PHYSICS)****THESIS ADVISORY COMMITTEE: PUANGPEN TANGBOONDUANGJIT, Ph.D.,  
PORNPAN YONGVITHISATID, M.Sc., CHIRAPHA TANNANONTA, M.Sc.****ABSTRACT**

Tumor moving due to respiration during the radiation treatment process is difficult to manage. Without management for respiratory motion, the critical organs may receive a high radiation dose with decreasing target dose. Synchrony<sup>®</sup> respiratory tracking of the Cyberknife system provides the unique possibility to do real-time patient and tumor motion tracking.

An in-house respiratory motion phantom was designed and constructed for testing the targeting accuracy of the Synchrony<sup>®</sup> system. To simulate target and skin respiratory motions, an in-house respiratory motion phantom ( $17 \times 45 \times 15 \text{ cm}^3$ ) made of acrylic was created. Inside the phantom, there were two parts; the mechanical part is composed of a cam and a slash cut pipe driven by a gear motor with 12 VDC to move the tumor and skin motion platform. The electrical part consists of AC to DC switching connected to an adjustable voltage regulator for supplying the gear motor. The amplitude and respiratory rate of the phantom were calibrated and evaluated using the Varian Real-Time Position Management (RPM) system. Then the phantom was used to test the targeting accuracy of the Synchrony<sup>®</sup> system by varying the amplitude of skin motion, respiratory rate, and tumor motion distance.

The phantom can be moved along the superior-inferior (SI) directions (tumor motion) with the distances of 15, 25, and 35 mm and moved along the anterior-posterior (AP) direction (skin motion) from 0 to 15 mm. The respiratory rates can be varied from 0 to 30 cycles/min. The maximum SD of amplitude and the respiratory rate in the phantom were 0.22 mm and 0.089 sec/cycle, respectively. The targeting error of the Synchrony<sup>®</sup> system is less than 1.0 mm. The skin motion amplitude, respiratory rate, and tumor distance don't affect the targeting accuracy of the system.

**KEY WORDS: CYBERKNIFE/ SYNCHRONY RESPIRATORY TRACKING SYSTEM/  
RESPIRATORY MOTION PHANTOM/ TARGETING ACCURACY**

63 pages.

การออกแบบและประดิษฐ์หุ่นจำลองการหายใจสำหรับทดสอบความถูกต้องของเป้าหมายของเทคนิคการติดตามการหายใจซินโครนีในเครื่องฉายรังสีศัลยกรรมท้าวร่างกายชนิดไซเบอร์ไนฟ์  
DESIGN AND CONSTRUCTION OF A RESPIRATORY MOTION PHANTOM FOR TESTING THE TARGETING ACCURACY OF THE CYBERKNIFE SYSTEM WITH THE SYNCHRONY<sup>®</sup> RESPIRATORY TRACKING SYSTEM

จิรศักดิ์ คำฟองเครือ 5036373 RAMP/M

วท.ม. (ฟิสิกส์การแพทย์)

คณะกรรมการที่ปรึกษาวิทยานิพนธ์ : พวงเพ็ญ ตั้งบุญดวงจิตร, Ph.D., พรพรรณ ยงวิทิศถิต,  
M.Sc., จีระภา ตันนานนท์, M.Sc.

#### บทคัดย่อ

ในกระบวนการฉายรังสีที่จัดการเกี่ยวกับก้อนเนื้ออกที่มีการเคลื่อนที่ตามการหายใจเป็นสิ่งที่ยุงยาก ซึ่งถ้าไม่มีการจัดการจะทำให้เนื้อเยื่อปกติได้รับปริมาณรังสีสูงขณะที่ก้อนเนื้ออกได้น้อยลง ในเครื่องฉายรังสีศัลยกรรมท้าวร่างกายชนิดไซเบอร์ไนฟ์มีระบบการติดตามการหายใจชนิดซินโครนีที่สามารถติดตามก้อนเนื้ออกที่มีการเคลื่อนที่ตามการหายใจแบบทันทีได้

ในงานวิจัยครั้งนี้ได้ออกแบบและประดิษฐ์หุ่นจำลองการหายใจที่จำลองก้อนเนื้ออกและการเคลื่อนที่ของการหายใจสำหรับทดสอบความถูกต้องของเป้าหมายของระบบการติดตามการหายใจชนิดซินโครนี โดยที่หุ่นจำลองสร้างจากแผ่นอะคริลิกขนาด  $17 \times 45 \times 15$  ซม. ซึ่งกลไกการขับเคลื่อนใช้เกียร์มอเตอร์ในการขับเคลื่อนและท่อนิวแมติกส์ทำให้เกิดการเคลื่อนที่ของแท่นก้อนเนื้ออกและผิวหนัง ในส่วนของอิเล็กทรอนิกส์ใช้เอซี/ดีซี สวิตชิงและวงจรรีเลย์เพื่อปรับความต่างศักย์ที่จ่ายกระแสไฟให้กับเกียร์มอเตอร์เพื่อให้เกิดการขับเคลื่อน โดยสามารถเปลี่ยนแปลงความเร็วได้ จากนั้นหุ่นจำลองได้ทำการสอบเทียบและประเมินโดยใช้ระบบอาร์พีเอ็มและมีการนำหุ่นจำลองมาทดสอบความถูกต้องของเป้าหมายของระบบซินโครนีโดยการเปลี่ยนแปลงขนาดของการหายใจ, อัตราเร็วของการหายใจและระยะของก้อนเนื้ออก

จากผลการทดลองพบว่าหุ่นจำลองการหายใจสามารถเคลื่อนที่ในแนวนอนล่าง (ก้อนเนื้ออก) เป็นระยะ 15, 25 และ 25 มม. เคลื่อนที่ในแนวหน้าหลัง (ขนาดการหายใจ) เป็นระยะ 0 ถึง 15 มม. และอัตราการหายใจสามารถปรับเปลี่ยนได้ตั้งแต่ 0 ถึง 30 ครั้งต่อนาที โดยที่ค่าเบี่ยงเบนมาตรฐานมากที่สุดในการเคลื่อนที่ในแนวหน้าหลังของขนาดการหายใจและอัตราเร็วในการหายใจมีค่า 0.22 มม. และ 0.089 วินาทีต่อรอบ ตามลำดับ ส่วนความคลาดเคลื่อนของเป้าหมายในระบบการติดตามการหายใจชนิดซินโครนีมีค่าน้อยกว่า 1 มม. และพบว่าขนาดของการหายใจ, อัตราเร็วของการหายใจและระยะของก้อนเนื้ออกไม่มีผลต่อความถูกต้องของระบบซินโครนี

## CONTENTS

	<b>Page</b>
<b>ACKNOWLEDGEMENTS</b>	<b>iii</b>
<b>ABSTRACT (ENGLISH)</b>	<b>iv</b>
<b>ABSTRACT (THAI)</b>	<b>v</b>
<b>LIST OF TABLES</b>	<b>vii</b>
<b>LIST OF FIGURES</b>	<b>viii</b>
<b>LIST OF ABBREVIATIONS</b>	<b>x</b>
<b>CHAPTER I INTRODUCTION</b>	<b>1</b>
<b>CHAPTER II OBJECTIVES</b>	<b>11</b>
<b>CHAPTER III LITERATURE REVIEWS</b>	<b>12</b>
<b>CHAPTER IV MATERIALS AND METHODS</b>	<b>16</b>
<b>CHAPTER V RESULTS</b>	<b>34</b>
<b>CHAPTER VI DISCUSSION</b>	<b>42</b>
<b>CHAPTER VII CONCLUSION</b>	<b>44</b>
<b>REFERENCES</b>	<b>45</b>
<b>APPENDICES</b>	<b>50</b>
Appendix A Cyberknife system	<b>51</b>
Appendix B Synchrony <sup>®</sup> respiratory tracking system	<b>53</b>
Appendix C Real-time Position Management <sup>™</sup> (RPM) System	<b>59</b>
Appendix D The E2E test (End to end test)	<b>61</b>
<b>BIOGRAPPHY</b>	<b>63</b>

## LIST OF TABLES

<b>Table</b>	<b>Page</b>
1.1 Lung tumor motion data	3
1.2 Abdominal tumor motion data	4
1.3 Correlation of tumor/organ motion with the respiratory signal	5
4.1 The parameter' values for testing the synchrony <sup>®</sup> respiratory tracking	32
5.1 The standard deviation of amplitude position (mm) of the in-house respiratory motion phantom	37
5.2 The standard deviation of respiratory rate (sec/cycle) of the in-house respiratory motion phantom	38
5.3 Total targeting errors (mm) of various amplitudes of skin motion for 15 cycles/min respiratory rate and 25 mm tumor motion distances	40
5.4 Total targeting errors (mm) of various respiratory rates for 7.5 mm amplitude of skin motion and 25 mm tumor motion distances	40
5.5 Total targeting errors (mm) of various tumor motion distances for 7.5 mm amplitude of skin motion and 15 cycles/min respiratory rate	40

## LIST OF FIGURES

<b>Figure</b>	<b>Page</b>
1.1 The Synchrony motion table and ball-cube assembly	6
1.2 Respiratory motion phantom modified by John et al.	7
1.3 Respiratory gating platform	7
1.4 Quasar™ respiratory motion phantom	8
3.1 Respiratory motion simulator	12
3.2 Test object for End to End test	13
3.3 The set up of the Optotrak certus in Cyberknife treatment room	14
4.1 3 and 5 mm thickness acrylic plates, PVC pipes and nut and bolt	16
4.2 Gear motor 12 VDC	17
4.3 Switching power supply	17
4.4 Adjustable voltage regulator circuit	18
4.5 Lead, Electric wire, Electric soldering iron and coping saw	18-19
4.6 Tourniquet	19
4.7 The external part of the phantom	20
4.8 Each part of the in-house respiratory motion phantom model	21
4.9 Top view of inside phantom	21
4.10 The electronic circuit diagram of the phantom	22
4.11 The constructions of in-house respiratory motion phantom	23
4.12 RPM system	24
4.13 XY/4D motion simulation table	25
4.14 Cyberknife machine in Ramathibodi hospital	26
4.15 The MultiPlan® treatment planning system	26
4.16 Computed tomography (CT) simulator machine in Ramathibodi hospital	27
4.17 The acrylic ball and the ball-cube rendering (b) The ball-cube assembly with precut MD55 gafchromic film	28

## LIST OF FIGURES (cont.)

<b>Figure</b>	<b>Page</b>
4.15 The in-house respiratory motion phantom	28
4.16 A flatbed transparency scanner	29
4.17 Treatment plan of the E2E test ball-cube	30
4.18 The setup of the in house respiratory motion phantom and ball cube	31
5.1 Each part of in-house Respiratory motion phantom	34
5.2 The completed in-house respiratory motion phantom	35
5.3 The amplitude position (mm) on the skin motion platform and respiratory rate position of the respiratory motion phantom.	36
5.4 Sinusoidal waves at amplitude position of 7.5 mm and respiratory rate of 15 cycles per minute of in-house respiratory motion phantom	37
5.5 The example of irradiated film and digital centroid analysis E2E software	36
1A Main component of Cyberknife robotic radiosurgery system	51
1B The Synchrony Respiratory Tracking System	53
2B Main components of the Cyberknife robotic radiosurgery system with the synchrony respiratory tracking system.	54
3B Three markers are attached to a snugly fitting vest that the patient wears during treatment	56
4B Illustration of phase difference and its effect on correlation between external marker and target positions.	57
1C The Real-time Position Management™ (RPM) System	60
1D The ball-cube phantom	61
2D Analysis software package provide by Accuracy for E2E test	62

## LIST OF ABBREVIATIONS

<b>Abbreviation</b>	<b>Term</b>
CTV	Clinical Target Volume
PTV	Planning target volume
mm	Millimetre
CT	Computed Tomography
MR	Magnetic Resonance
AP	Anterior-posterior
LR	Left-right
SI	Superior-inferior
et al.	et alii (Latin) - and others
3D	Three-dimensional
etc.	et cetera (Latin) - and other things
MRI	Magnetic resonance imaging
s	Second
2D	Two-dimensional
DC	Direct current
AC	Alternating current
AC/DC	Alternating current to Direct current
i.e.	id est (Latin) - that is
e.g.	exempli gratia (Latin) -for example
Linac	Linear accelerator
TLS	Target locating system
SAD	Source-to-Axis Distance
cm	Centimetre
kV	Kilovoltage
kVp	Kilovoltage peak
Amp, mA	Ampere, Milliampere

## LIST OF ABBREVIATIONS (cont.)

<b>Abbreviation</b>	<b>Term</b>
ms	Millisecond
MV	Megavoltage
cGy	Centigray
GHz	Gigahertz
DRRs	Digitally reconstructed radiographs
RTS	Respiratory tracking system
LEDs	Light Emitting Diodes
CCD	Charge coupled device
PC	Personal computer
RPM	Real-time Position Management
IR	Infrared
E2E	End to end test
SMS	Skin Motion Simulator
TMS	Tumor Motion Simulator
PVC	Polyvinyl chloride
VDC, VAC	Voltage direct current, Voltage Alternating current
W	Watt
cm <sup>2</sup>	Centimeter squared
cm <sup>3</sup>	A cubic centimetre or cubic centimeter
PSU	Power supply unit
Dpi	Dots per inch
min	Minute
ANOVA	Analysis of Variance
CI	Confidence interval

## **CHAPTER I**

### **INTRODUCTION**

The optimized radiation therapy is to precisely deliver a lethal dose to the target volume while minimizing the dose to surrounding healthy tissues and critical structures [1, 2]. Moving target volume is complicated to fulfill this objective, it is well known that target motion due to breathing is one of the major obstacles in dose escalation of radiation therapy to some tumors in the thoracoabdominal region [3]. Thus respiratory motion is a significant and challenging problem in radiation therapy [4]. Several approaches have been developed to manage the effect of respiratory motion in radiation oncology [5]. The conventional method of increasing the internal margin component of the clinical target volume (CTV) is almost always used to increase the volume of healthy tissues exposed to high doses that consequently increases the likelihood of treatment-related complications [6]. Furthermore, reduction of respiratory motion can be achieved by using either breath-hold techniques or respiratory gating techniques. However, the disadvantage of both techniques is the increasing of treatment time. Another way to manage respiratory motion better but also more difficult approach is to allow patient to breathe freely while a tracking and control systems monitor the tumor's position and the position of external markers, Synchrony<sup>®</sup> respiratory tracking system, the tumor position is inferred from the external breathing surrogates. The Synchrony<sup>®</sup> system is a respiratory compensation system integrated to Cyberknife<sup>®</sup> (Accuray Inc.), which uses external markers in conjunction with diagnostic x-ray imaging to compensate for respiratory motion [7, 8]. Then, evaluations of accuracy of Synchrony<sup>®</sup> respiratory tracking system should be considered to be full of confidence that it can be able to maximize tumor control probability while minimize normal tissue complication. As a result, it will decrease the mortality and improve the quality of life.

## 1.1 Magnitude and measurement of respiratory motion

Intrafraction motion can be caused by the respiratory, skeletal muscular, cardiac and gastrointestinal systems. Of these four systems, it is well known that respiration induced anatomic motion is an important source of positional, or geometric, uncertainty in organs of the thorax and abdomen [9, 10]. This intrafraction motion impacts all forms of external beam radiation therapy and is an issue that becomes increasingly important in the era of image guided radiation therapy (IGRT) [5].

Respiratory motion affects all tumor sites in the thorax and abdomen, including in particular the lung, liver, pancreas, kidneys, and other thoracic and abdominal tumor which can move as much as 35 - 40 mm [5-7, 11, 12]. Quetelet (1842) and Hutchinson (1850) studied the pattern of breathing on 300 and 1714 adult subjects, respectively. Their data show very wide frequency range, between 6 and 31 times per minute [13]

At rest with normal situation, a healthy person breathes 12 to 15 times per minute [14] and the movement amplitudes of individual skin respiratory motion markers range from 3.1 to 14.8 mm with a median of 7.5 mm [15]. The motion also varies markedly between patients, indicating that an individual approach to respiratory management is advised.

Internal organ motion has been detected via ultrasound, computed tomography (CT), magnetic resonance (MR), nuclear medicine and fluoroscopy. The respiratory motion studies have tracked the movement of the tumor with the radiographic of internal markers embedded at the tumor site. These data are summarized in tables 1.1 and 1.2 for lung and abdominal tumor motion, respectively.

**Table 1.1** Lung tumor motion data showing the ranges (minimum- maximum) and mean values in millimeters for each site in three dimensions; AP: anterior-posterior; LR: left-right; SI: superior-inferior [9].

Observer	Direction		
	SI	AP	LR
Barnes: Lower lobe	18.5 (9-32)	-	-
Middle, upper lobe	75 (2-11)	-	-
Chen	(0-5)	-	-
Ekberg	3.9 (0-12)	2.4 (0-5)	2.4 (0-5)
Engelsman:			
Middle/upper lobe	(2-6)	-	-
Lower lobe	(2-9)	-	-
Erridge	12.5 (6-34)	9.4 (5-22)	7.3 (3-12)
Ross:	-	1 (0-5)	1 (0-3)
Middle lobe	-	0	9 (0-16)
Lower lobe	-	1 (0-4)	10.5 (0-13)
Grills	(2-3)	(0-10)	(0-6)
Hanley	12 (1-20)	5 (0-13)	1 (0-1)
Murphy	7 (2-15)	-	-
Plathow: Lower lobe	9.5 (4.5-16.4)	6.1 (2.5-9.8)	6.0 (2.9-9.8)
Middle lobe	7.2 (4.3-10.2)	4.8 (1.9-7.5)	4.3 (1.5-7.1)
Upper lobe	4.3 (2.6-7.1)	2.8 (1.2-5.1)	3.4 (1.3-5.3)
Sppenwoolde	5.8 (0-25)	2.5 (0-8)	1.5 (0-3)
Shimizu	-	6.4 (2-24)	-
Sixel	(0-13)	(0-5)	(0-4)
Stevens	4.5 (0-22)	-	-

**Table 1.2** The ranges (minimum- maximum) and mean of abdominal tumor motion in millimeters for each site in the superior-inferior (SI) direction [9].

Site	Observer	Breathing mode	
		Shallow	Deep
Pancreas	Suramo	20 (10-30)	43 (20-80)
	Bryan	20 (0-35)	-
Liver	Weiss	13 $\pm$ 5	-
	Harauz	14	-
	Suramo	25 (10-40)	55 (30-80)
Kidney	Davies	10 (5-17)	37 (21-57)
	Suramo	19 (10-40)	40 (20-70)
	Davies	11 (5-16)	-
Diaphragm	Wade	17	101
	Korin	13	39
	Davies	12 (7-28)	43 (25-57)
	Weiss	13 $\pm$ 5	-
	Giraud	-	35 (3-95)
	Ford	20 (13-31)	-

From the data, the lung tumor motions generally show a much greater variation. The most motion of the abdominal values is the superior-inferior (SI) direction and no more than a two millimeters displacement in the anterior-posterior (AP) and lateral directions.

The amount of a lung tumor position moving during breathing varies widely. Stevens et al. found that no correlation between the occurrences or magnitude of tumor motion and tumor size, location, or pulmonary function. They suggested that tumor motion should be assessed individually.

In magnitudes of respiratory motion, there are no general patterns of respiratory behavior that can be assumed for a particular patient prior to observation and treatment. Many individual characteristics of breathing; quiet versus deep, chest

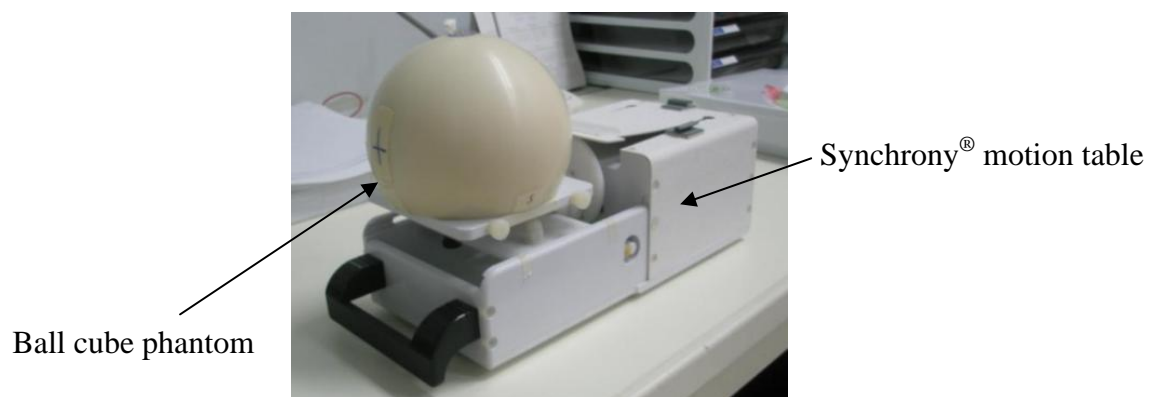
versus abdominal, healthy versus compromised, etc. and many motion variations associated with tumor location and pathology lead to individual patterns in displacement, direction, and phase of tumor motion. Thus, the correlation of respiratory motion between tumor motion with radiographic internal markers (fiducials) embedded at the tumor site and organ motion with respiratory signal are studied and illustrated schematically in table 1.3.

**Table 1.3** Correlation of tumor/organ motion with the respiratory signal [9].

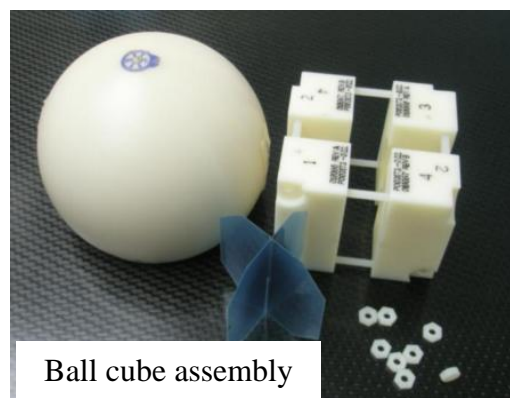
Organ/Source	Respiratory signal	N patient (measurement)	Correlation	Phase shift	Source
Diaphragm SI fluoroscopy	Abdominal displacement	5 (60)	0.82-0.95	Not observed	Vedam et al(16)
Tumor and diaphragm, fluoroscopy	Abdominal displacement	43	0.41-0.94	Short delays observed	Ahn et al. (12)
Tumor, SI fluoroscopy	Spirometry and abdominal displacement	11 (23)	0.39-0.99	-0.65-0.5 s	Hoisak et al. (17)
Tumor, 3D biplane radiography	Abdominal displacement	26	Respiratory waveform cycle agree with SI and AP tumor motion	Principally with 0-0.3 s existence of > 1.0 s	Tsunashima et al. (18)
Lung vessel, cine MRI	Abdominal displacement	4	SI $0.87 \pm 0.23$ AP $0.44 \pm 0.27$	-	Koch et al. (19)
Lung tumor, Respiration-correlation CT	Abdominal displacement	9 where tumor SI motion > 5mm	0.74-0.98	<1 s 4pts	Mageras et al. (10)
Lung tumor, SI respiration-correlation CT	Diaphragm position	12	0.73-0.96	<1 s 4pts <0.5 s 5 pts	Mageras et al (10).

## 1.2 The simulation of respiratory motion

Many types of respiratory motion phantom are built for evaluating the efficiency and accuracy of respiration correlated radiation therapy technique. The Cyberknife manufacturer invented a Synchrony<sup>®</sup> motion table as shown in figure 1.1. It is a 2D motion phantom using DC motor and cam for the driving force with variable speed, one moving along the superior to inferior direction (longitudinal axis) that referred to target motion and another moving along the anterior to posterior direction (vertical axis) that referred to skin respiratory motion. It was used in the verification of the proper operation of Synchrony<sup>®</sup> tracking system at a clinical site. This done by comparing the targeting accuracy and dose distribution of treatment planning and true field of radiation of ball cube phantom, will be measured both positioning accuracy and radiation distribution shape [20].



(a)



(b)

**Figure 1.1** (a) The Synchrony<sup>®</sup> motion table and (b) ball-cube assembly

John et al modified a standard respiratory motion phantom tool with an AC/DC device that allowed setting of constant full cam rotation time of 4 seconds. Second identical cam was added which will have the phantom block to move in the left and right direction of 25 mm distance as shown in figure 1.2 [21].

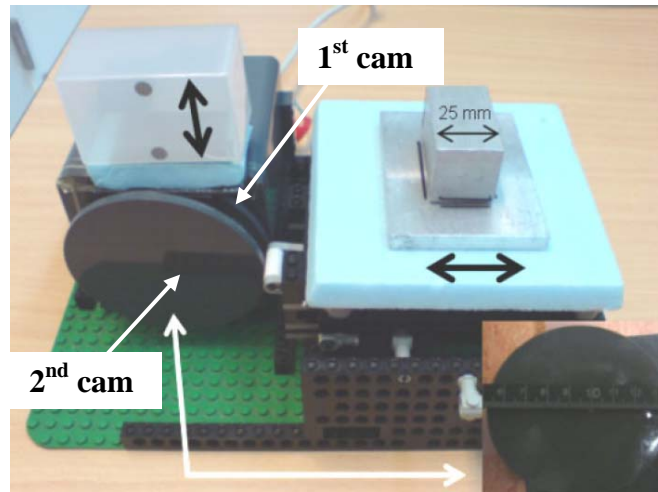


**Figure 1.2** Respiratory motion phantom modified by John et al

The Standard Imaging Inc. invented a respiratory gating platform as illustrated in figure 1.3 to simulate the breathing motion along the longitudinal axis of over a 5 mm to 40 mm distance to replicate tumor motion. Cycle interval or respiratory rate can be varied from 2.0 to 6.0 seconds per cycle, independently control the range of motion and the respiratory cycle [22].



**Figure 1.3** Respiratory gating platform

The Modus Medical devices Inc. has produced the Quasar™ respiratory motion phantom shown in figure 1.4. The cylinder motion occurs in superior-inferior direction from 0 to 40 cm and respiratory rate can be varied from 4 to 50 cycles per minute. A platform which refers to skin motion is the same respiratory rate as cylinder, an amplitude of skin motion is moved with 1 cm (anterior to posterior direction) [23].



**Figure 1.4** Quasar™ respiratory motion phantom

### **1.3 Methods to account for respiratory motion in radiotherapy**

Several methods have been developed to manage the effect of respiratory motion in radiation therapy [5]. One is to enlarge the clinical target volume (CTV) by increasing margin of tumor positions during respiration, a related motion-encompassing approach is the slow CT scanning method or multiple CT scans are averaged that multiple respiration phases are recorded per slice (maximum intensity projection) that the images of the tumor show the full extent of the respiratory motion. But the disadvantage of slow CT scan methods is the loss of resolution due to motion blurring and the increased dose from slow CT scanning. Although this method will not affect the dose delivered to the target, it will also lead to increase dose delivered to normal tissues or critical organ.

Another method to minimize the PTV margin is the breath-hold method that minimizes the effects of respiratory motion on radiation treatment, typically

applied at normal end - exhalation or deep inhalation. This method provide higher accuracy of dose delivery to target than motion-encompassing methods, but breath holding is not applicable to most patients due to compliance, especially for elderly patients or patients with compromised pulmonary capacity.

For respiratory gating methods that allows the patient to breathe normally with the radiation beam is turned on only within a specified portion (phase or amplitude) of the patient's respiratory cycle. The position and width of the respiratory gating are determined by monitoring the patient's respiratory motion using either an external respiratory signal to infer the tumor position, or by directly tracking implanted radio-opaque markers (fiducials) fluoroscopically. Typically the gate is chosen over a range of the respiration cycle during which the tumor motion is minimal (at exhale) or the lung volume is maximal (at inhale). Gating does allow a reduction of the PTV margin resulting in decrease dose to normal tissue. However, the disadvantage of respiratory gating is limited portion of the breathing cycle which can reduce the duty cycle (the fraction of the gate width to the respiratory cycle period), increase the treatment time [2, 5, 6, 9, 24].

Another method to manage the effect of respiratory motion is to move or shape the radiation beam dynamically to target; this will be referred to as real-time tracking system. Under ideal condition, continuous real-time tracking can reduce the tumor motion margin in dose distribution while maintaining a 100% duty cycle for efficient dose delivery [5, 9, 25]. Real-time tracking requires the ability to automatically adjust the position of the beam relative to the moving target. There are four possible ways to do this:

- (a) Shift the patient using a remotely controlled couch.
- (b) Shift the aperture of a remotely controlled collimator (Multileaf collimator).
- (c) Redirect the beam electromagnetically (for charged-particle beams).
- (d) Shift the beam by physically repositioning the radiation source (i.e., a linear accelerator).

All of these methods require connecting a system for measuring tumor position through a real-time control loop to the beam alignment system. Because moving tumors have more degrees of freedom than a conventional gantry-mounted

linear accelerator (Linac) and couch, real-time tracking requires specialized beam/patient positioning tools [5, 25]. Thus to succeed, a tracking system must be able to do four things:

- (a) Determination of the tumor position
- (b) Anticipation of the tumor motion to allow for time delays in realignment of the beam
- (c) Transmittal of the target coordinates to the re-alignment system through a control loop
- (d) Reposition of the beam

All of these must be done automatically and in real time, where real time refers to timescales that are short compared to the period over which the tumor moves appreciably [9, 24, 26].

If the tumor position must be inferred from the respiratory surrogate's motion such as the chest or abdomen, the control loop also requires an algorithm that relates tumor to surrogate motion which the most general and robust surrogate tracking algorithm should adapt to changes in the respiration patterns. This is the basis of the Cyberknife with Synchrony respiratory tracking system [26] (appendix A and B).

## **CHAPTER II**

### **OBJECTIVES**

The main purpose of this experiment was to construct a respiratory motion phantom for testing the targeting accuracy of the Synchrony<sup>®</sup> respiratory tracking system.

The other two sub-purposes were:

1. To evaluate the targeting accuracy of the Synchrony<sup>®</sup> respiratory tracking system.
2. To study the correlation of the amplitude of skin motion, respiratory rate and moving distance of tumor with the total targeting errors in the Synchrony<sup>®</sup> respiratory tracking system.

## CHAPTER III

### LITERATURE REVIEWS

T. Zhou, et al [27] developed a respiratory motion phantom simulator as shown in figure 3.1. It consists of two independent programmable robotic 3D linear motion platforms, Skin Motion Simulator (SMS) and Tumor Motion Simulator (TMS). The SMS consists of three high-precision orthogonally mounted linear slides, and the TMS consists of two such linear slides and one vertically mounted linear piston actuator (Ultra Motion, LLC). Each stage includes a high-performance servomotor, an integrated gear head at the motor output shaft, and an optical rotary encoder mounted on the motor back shaft. The platforms are controlled by a personal computer through an Ethernet-addressable motion control board. The simulated motions were evaluated by using Optotrak, which was placed about two millimeters from the simulator. For each test, two sets of data were collected: one set measured the motion at the top stage of the simulator in Optotrak's coordinates and the other measured the commanded motion to each slide in the simulator's coordinates. A registration method was applied to convert the Optotrak results into the simulator's coordinates for comparison. As a result, respiratory skin and tumor motions have a precision better than  $\pm 0.1$  mm that will be a tool in Cyberknife suited for phantom treatments, dose verifications of Synchrony<sup>®</sup> respiratory system.

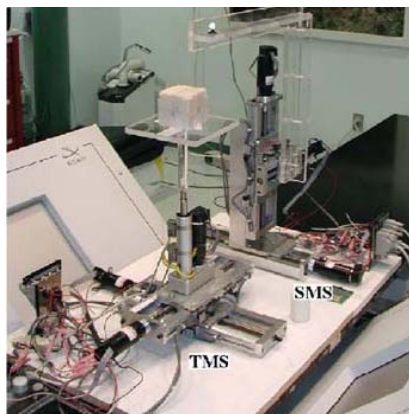


**Figure 3.1** Respiratory motion simulator

Researchers from three Cyberknife centers [28] studied the Synchrony<sup>®</sup> respiratory tracking system. They conducted an “end-to-end” test procedure using a test object to simulate a spherical target as shown in figure 3.2. Orthogonal radiochromic films can be placed within the test object, which allows for subsequent comparison of planned and delivered a spherical dose profiles. After irradiation, a film analysis software package provided by Accuray calculates the centroid of the delivered dose profiles. The distance between the centers of the planned and delivered dose profiles is a measure of the system’s submillimeter accuracy and thus represents all possible errors in the treatment planning and delivery process including error in the tracking system. Programmable motion tables were used to simulate respiratory motion of the object and the external optical markers, the amplitude of motion was 25, 8, and 3 mm for superior-inferior, anterior-posterior, and left-right directions, respectively. The motion pattern was a sine<sup>4</sup> ( $\omega T/2$ ) waveform; the period was 3.6 s; and the phase difference between the object and marker motions was 0, 15, and 30 degrees for different experiments. As a result, the mean error observed during treatment with the Synchrony<sup>®</sup> system across all motion patterns was  $0.7 \pm 0.3$  mm.

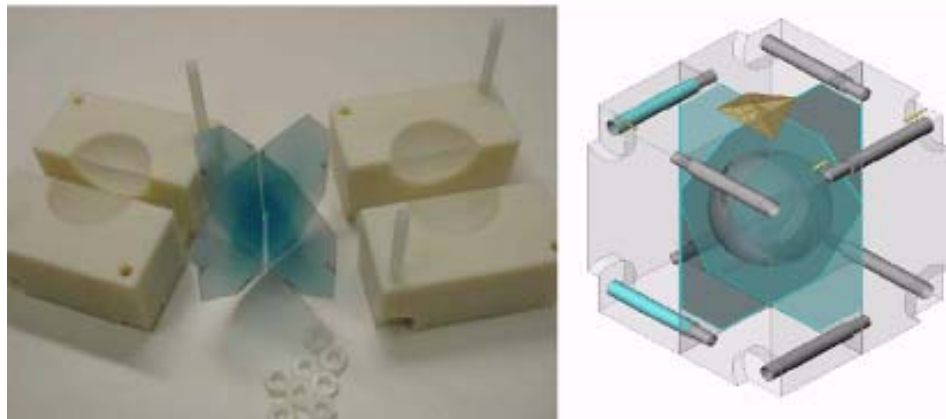


**Figure 3.2** Test object for End to End test

K Wong, et al [4, 29] studied the accuracy and precision of the beam steering by recording the motions of both the Linac and a ball-cube target using an independent optical tracker in the Synchrony<sup>®</sup> system. For this study, the target is a plastic ball-cube phantom which was scanned and planned for a 30 Gy at 100%

isodose line treatment. Respiratory motion was generated using a computer-controlled 3D motion simulator in regular respiratory motion as three sinusoids with the following extents: 10 mm SI, 10 mm AP, and 5 mm LR. The respiratory period was 5 seconds. All three axes were in phase. The Optotrak Certus optical tracking system for measurements in this study was used (Active LEDs were attached to the Linac and the motion simulator) as shown in figure 3.3. As a result, their findings summarized that Synchrony® was able to track 61 of the 98 beams. Inability to track occurred when the Optotrak view was blocked by the Linac or robot arm, or when the Linac was oriented in such a way that the markers on the end of the Linac were not visible to the Optotrak. The standard deviation of the Linac to target distance was  $0.82 \pm 0.27$  mm and these measurements provide independent, high-precision measurement of the tracking accuracy of Cyberknife with Synchrony® system



**Figure 3.3** The set up of the Optotrak certus (Arrow) in Cyberknife treatment room. Two LEDs are attached to the tumor motion simulator near the target ball-cube. An additional six LEDs are attached to the final collimator of the Cyberknife Linac.

G Kim, et al [30] evaluated the tumor motion and treatment accuracy of the Synchrony® tracking system for the treatment of liver motion. The motions of

tumor in 64 treatments of 24 patients were analyzed by using correlation error (the distance between the model-based estimated and image-based actual position) of log file in Synchrony® tracking system. As a result, the mean correlation error was  $1.1 \pm 0.7$  mm. It was shown that Synchrony motion tracking system has a clinically relevant accuracy in liver tumor.

## CHAPTER IV

### MATERIALS AND METHODS

For good communication, both material and method parts were reported in three parts. The first one is the design and construction of an in-house respiratory motion phantom. In the second part, the completed phantom was calibrated and evaluated with Real-time Position Management (RPM) system and the last one describes the application of the phantom in verify the targeting accuracy of the Synchrony® respiratory tracking system.

#### 4.1 Design and construction of the in-house respiratory motion phantom

##### 4.1.1 Materials

4.1.1.1 Acrylic plates, PVC pipe, nut and bolt (as shown in figure. 4.1 a, b, and c, respectively)



(a)



(b)



(c)

**Figure 4.1** (a) 3 and 5 mm thickness acrylic plates (b) PVC pipes (c) nut and bolt

#### 4.1.1.2 Gear motor

The gear motor with 12 VDC 15 Watt was used in the research. The speed of motor can be increased up to 50 rounds per minute. The dimension of its front area is  $6 \times 6 \text{ cm}^2$  with 8 mm axle (Figure 4.2).



**Figure 4.2** Gear motor 12 VDC

#### 4.1.1.3 Switching power supply

The switching power supply shown in figure 4.3 is an electronic power supply unit (PSU) with a switching regulator in order to provide the required DC output voltage. Its input voltage is 220 VAC with the output of 13.8 VDC - 10 Amp.



**Figure 4.3** Switching power supply

#### 4.1.1.4 Electronic board and parts for assembling an adjustable voltage regulator circuit

The adjustable voltage regulator circuit is important to convert the 13.8 VDC source to various DC voltages. This circuit is called a DC to DC converter or a voltage regulator. Figure 4.4 shows the electronic board and parts of the adjustable voltage regulator.

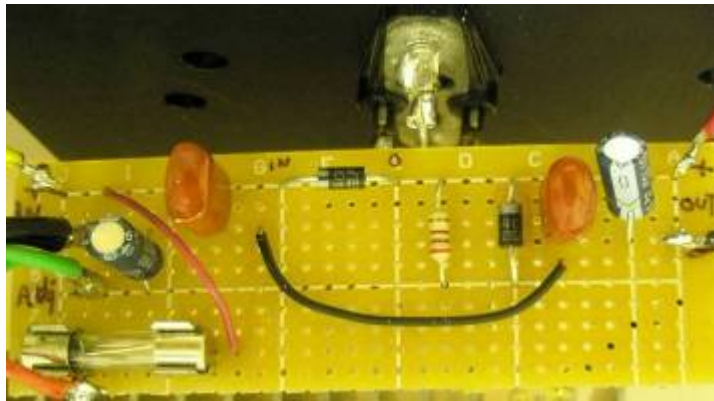


**Figure 4.4** The adjustable voltage regulator circuit

#### 4.1.1.5 Accessories for electronics

Figure 4.5 (a – d) shows the lead, electric wire and electric soldering iron used for connection of electronic circuit elements and coping saw (a type of hand saw used for cutting the acrylic plate and PVC pipes).



(a)



(b)



(c)



(d)

**Figure 4.5** (a) Lead (b) Electric wire (c) Electric soldering iron (d) coping saw

#### 4.1.1.6 Tourniquet

The tourniquet is a constricting device used to pull the tumor motion platform for moving in SI direction.

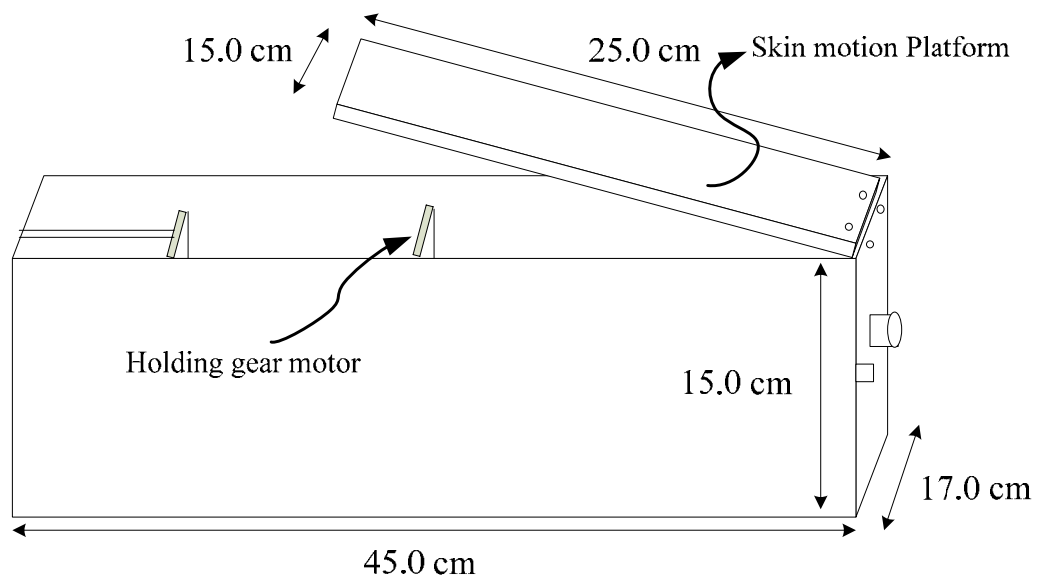


**Figure 4.6** Tourniquet

#### 4.1.2 Methods

The in-house respiratory motion phantom model was designed to be able to simulate respiratory motion signal and tumor motion.

The acrylic plates with 5 mm thickness were used for fabricating an external part of the phantom and 3 mm for the skin motion platform (Figure 4.7) and holding the gear motor and also supporting two long sides of the phantom. The nuts and bolts were used to join every part together. The size of the phantom is  $17 \times 45 \times 15 \text{ cm}^3$ .



**External Structure**

**Figure 4.7** The external part of the phantom

Inside the phantom, there are mechanical and electronic parts. The mechanical part was made of 3 mm thickness acrylic plate which consists of a skin motion platform (Figure 4.7), a tumor motion platform (Figure 4.8a), slashed PVC pipes with 15, 25, and 10 mm long (Figure 4.8b), and cam (Figure 4.8c).

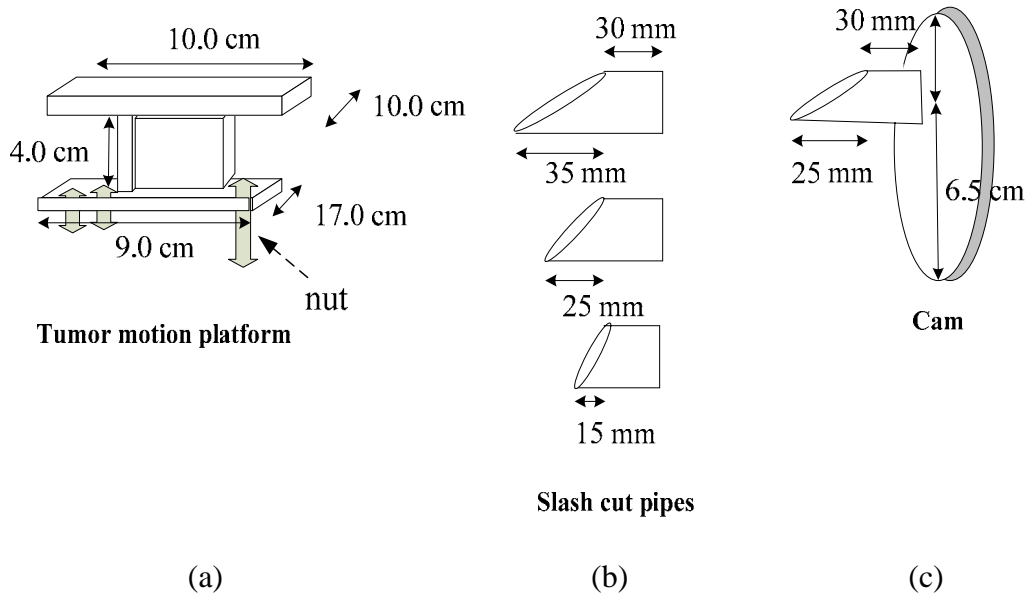


**Figure 4.8** Each part of the in-house respiratory motion phantom model

One end of slashed pipe was attached with the cam and another end attached with the tumor motion platform (Figure 4.9) by using four nuts and bolts to move the platform in supero-inferior (SI) direction with the same length of the pipe. (The tumor motion platform can move by push of slash cut pipe and pull with tourniquet). Moreover, another side of the cam was attached with the gear motor to rotate the cam for moving the skin motion platform in antero-posterior (AP) and tumor motion platform in SI direction.

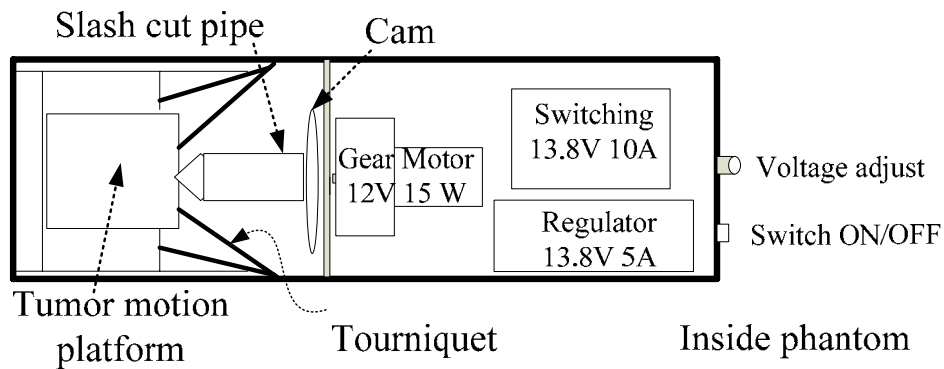


**Figure 4.9** Top view of inside phantom

The electronic part was composed of an adjustable voltage regulator circuit shown in figure 4.4. The circuit was assembled according to the circuit diagram illustrated in Figure 4.10.

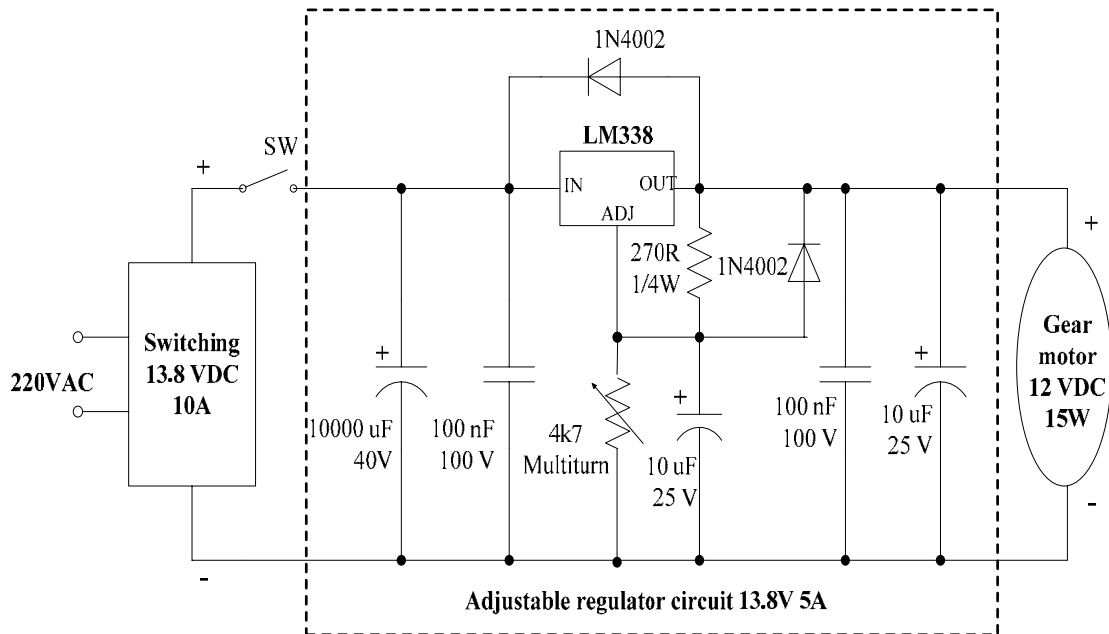


**Figure 4.10** The electronic circuit diagram of the phantom

The switching power supply convert the 220 VAC to 13.8 VDC and transfer the DC current to the adjustable voltage regulator circuit for driving gear motor with variable velocity adjusted by voltage regulator circuit. The construction of the respiratory motion phantom was shown in figure 4.11.

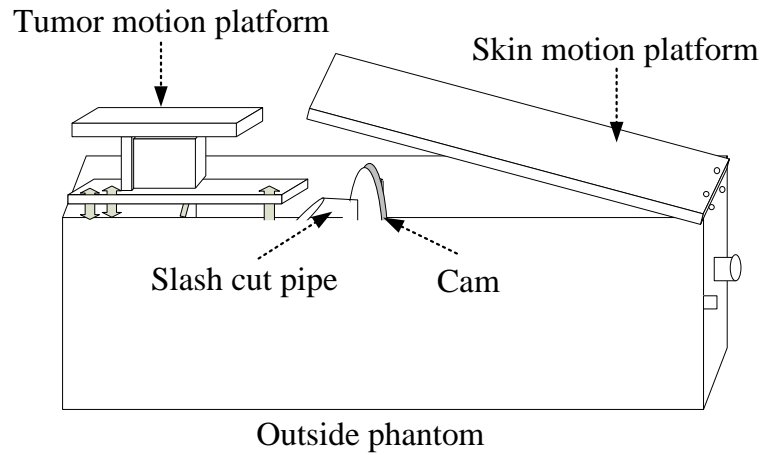


**Figure 4.11** The construction of the in-house respiratory motion phantom

## **4.2 Calibration and evaluation of the in-house respiratory motion phantom**

### **4.2.1 Materials**

The Real-time Position Management™ (RPM) system (appendix C)

The Real-time Position Management™ (RPM) system of Varian Medical Systems, Palo Alto, CA version 1.7.5 was used to monitor and record a respiratory signal, specifically the rise and fall of the anterior abdominal surface. The RPM system consists of Charge-Coupled Device (CCD) with illuminator ring, in-room viewfinder, junction box, marker block with infrared reflective two dots, and RPM workstation.

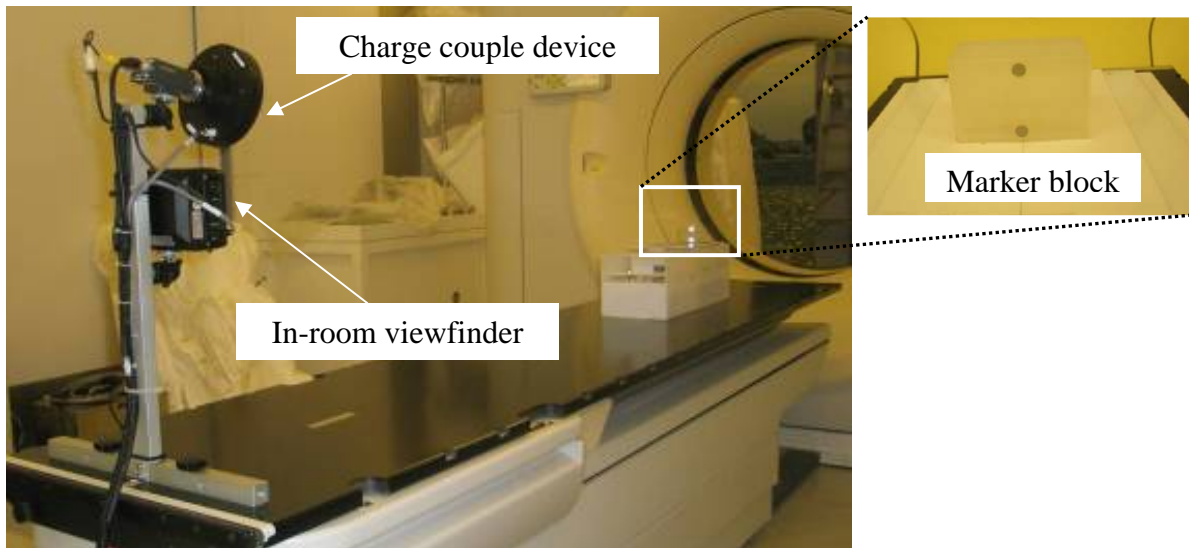


**Figure 4.12** The RPM system of Varian that consists of a Charge-Coupled Device (CCD) with illuminator ring, in-room viewfinder and marker block.

#### 4.2.1 Methods

In order to calibrate and evaluate the performance of the respiratory motion phantom, The RPM system was used to verify the amplitude and respiratory rate position.

Before the RPM system was used for calibration and evaluation of the phantom, it was verified by XY/4D motion simulation table of Sun Nuclear Corporation shown in figure 4.13. The simulation table has a respiratory surrogate housing which can move in AP direction to simulate skin motion. The respiratory surrogate housing can control the moving with computer software. For testing the RPM system, the respiratory signal with 20 mm amplitude and 4 sec/cycle respiratory rate was created. The standard deviation of amplitude and respiratory rate were calculated. The result shows the acceptable errors of less than 0.1 mm and 0.1 sec per cycle for amplitude and respiratory rate, respectively.

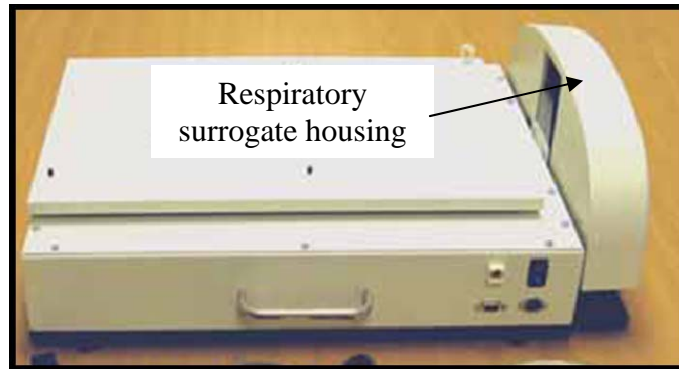


**Figure 4.13** XY/4D motion simulation table

The respiratory phantom surface motion was calibrated for the amplitude positions of 6, 7.5, 9, 12, and 15 mm and respiratory rates of 5, 10, 15, 20, 25, and 30 cycles per minute by placing the RPM block on the skin motion platform. The two circular markers on the block were track the infrared reflecting from the charge couple device (CCD).

The precision test of respiratory phantom was performed for the amplitude position of 7.5 mm for every respiratory rate and respiratory rate of 15 cycles per minute for every amplitude position.

### **4.3 Testing the targeting accuracy of Synchrony<sup>®</sup> respiratory tracking system**

#### **4.3.1 Materials**

4.3.1.1 Cyberknife with the Synchrony<sup>®</sup> respiratory tracking system

Figure 4.14 shows the Cyberknife machine with 6 MV photon beam and the Synchrony<sup>®</sup> respiratory tracking system with 4<sup>th</sup> generation (Accuracy Incorporated) of the Faculty of Medicine, Ramathibodi Hospital used for this study. The sizes of the secondary collimators of the machine are 5, 7.5, 10, 12.5, 15, 20, 25, 30, 35, 40, 50, and 60 mm diameters.



**Figure 4.14** Cyberknife machine in Ramathibodi Hospital

#### 4.3.1.2 Treatment planning system

The MultiPlan<sup>®</sup> treatment planning system of Cyberknife robotic radiosurgery system version 2.2 shown in figure 4.15 which was used for this study.



**Figure 4.15** The MultiPlan<sup>®</sup> treatment planning system

#### 4.3.1.3 Computed tomography (CT) simulator machine

The Philips Mx8000IDT - 16 CT scanner (Phillips Medical, Best, The. Netherlands) of the Faculty of Medicine, Ramathibodi Hospital shown in figure 4.16 was used for this study.

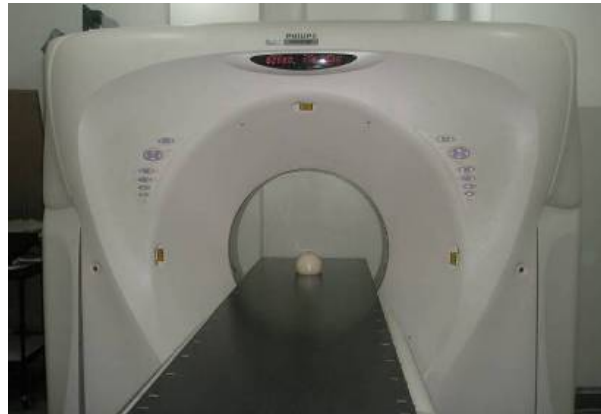
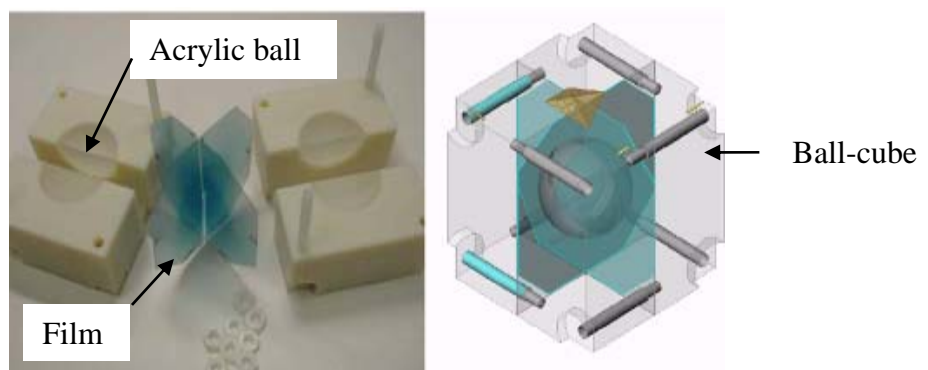


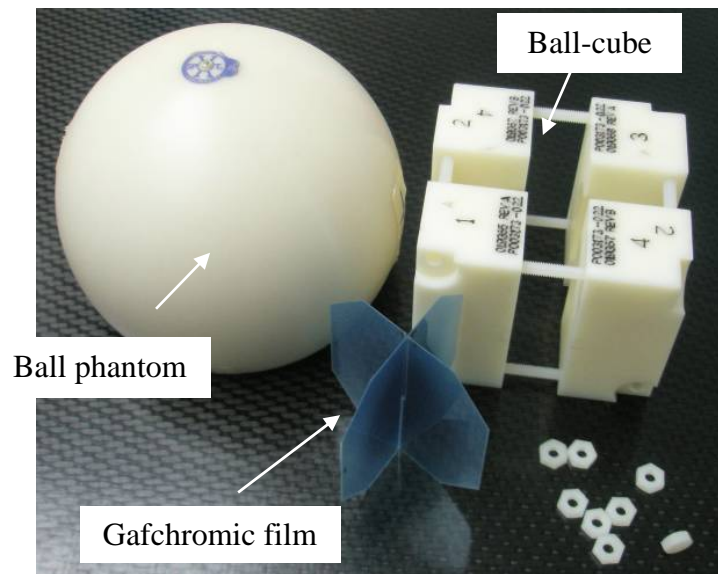
**Figure 4.16** Computed tomography (CT) simulator machine in Ramathibodi Hospital

#### 4.3.1.4 Ball-cube assembly with radiochromic

The ball cube is a targeting tool made of 4 pieces which connect together using threaded nylon rod and nuts. An acrylic ball with 31.75 mm diameter representing a target is placed in the center of the cube as shown Fig 4.17a. Two pieces of radiochromic film may be inserted perpendicularly together for dose distribution measurement. The ball-cube is placed in a plastic ball phantom (Fig. 4.17b). There are five metal fiducials inside the ball phantom for tracking process.



(a)



(b)

**Figure 4.17** (a) The acrylic ball and the ball-cube rendering (b) The ball-cube assembly with precut MD55 gafchromic film

#### 4.3.1.5 The in-house respiratory motion phantom

Figure 4.18 shows the in-house respiratory motion phantom for testing the targeting accuracy of the Synchrony<sup>®</sup> respiratory tracking.



**Figure 4.18** The in-house respiratory motion phantom

#### 4.3.1.6 A flatbed transparency scanner

A flatbed transparency scanner, Epson Perfection V700 Photo scanner (Fig.4.19) was used for this study. The size of scanning surface is 20 x 30 cm with the maximum resolution of the film scanning of 6400 dpi. .



**Figure 4.19** A flatbed transparency scanner

### 4.3.2 Methods

#### 4.3.2.1 CT Simulation and treatment planning

- a. A ball-cube with two pieces of film inside was loaded into the ball phantom with proper orientation (SI directions).
- b. The phantom was scanned by using axial mode, 120 kVp, and 1.5 mm slice thickness.
- c. The CT images of the ball-cube phantom were imported to the treatment planning system.
- d. In fiducial mode, every fiducial in the images was digitized.
- e. A treatment plan was generated with the goal of 80% isodose line of 6.5 Gy conforming the outer surface of the acrylic ball target (left = 31.75 mm, anterior = 31.75 and superior = 31.75 mm) with its center at the same point of the ball's as illustrated in figure 4.20.

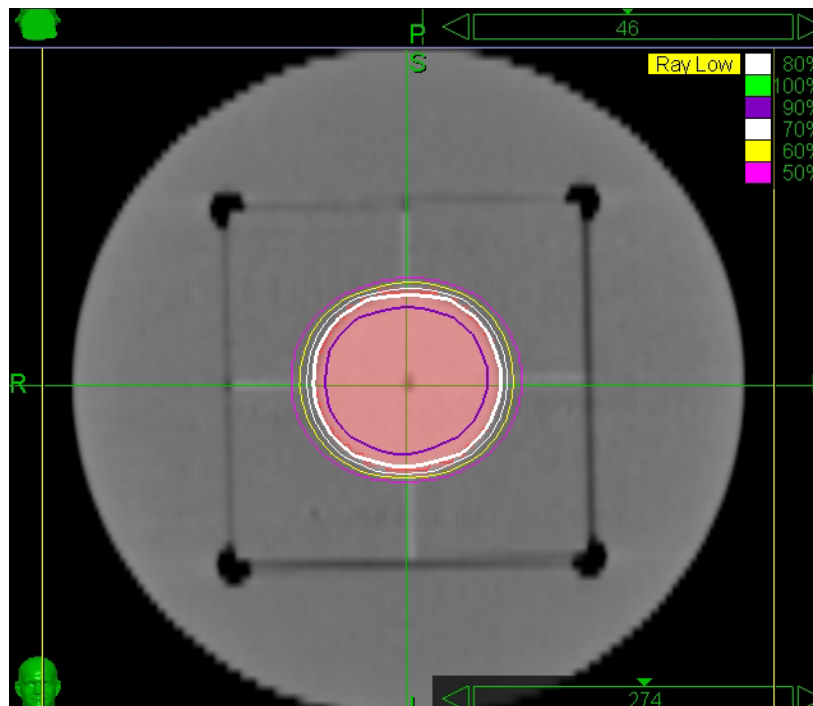


**Figure 4.20** The treatment plan for the E2E test ball-cube phantom

#### 4.3.2.2 Radiation Delivery

a. Digital reconstruction radiographs (DRRs) was generated to verify the treatment delivery.

b. The ball-cube with two pieces of MD55 Gafchromic film was placed on a piece of a 5 cm thick Styrofoam and then placed on the top of the tumor motion platform of the in-house respiratory motion phantom put on the treatment couch as shown in Figure 4.21. The orientation of anterior, superior and left edges of the film was marked on both pieces of the film. The setup orientation of the ball-cube in the phantom must be exactly the same as the CT scanning. .

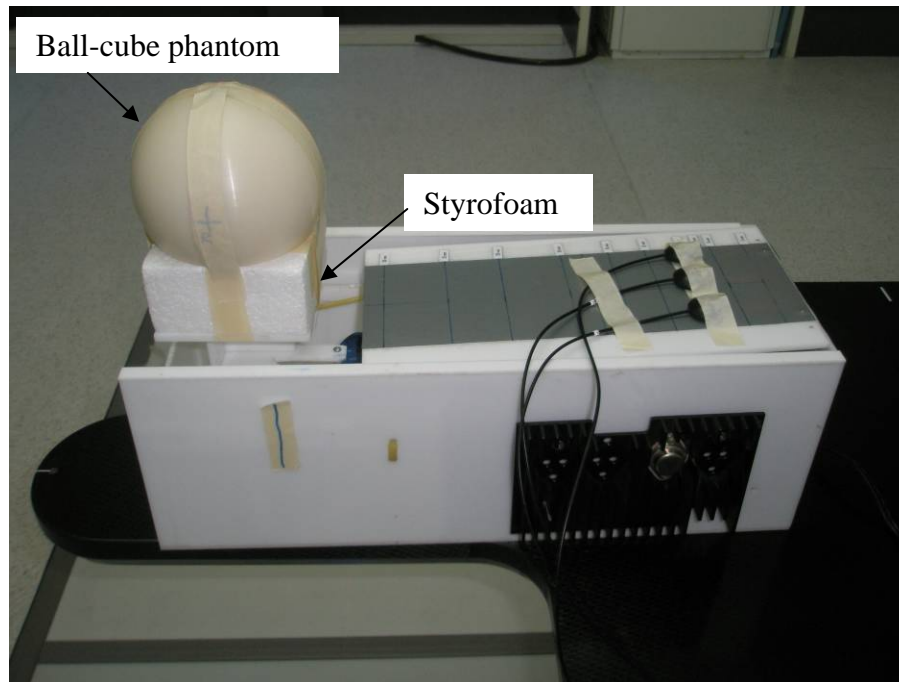


**Figure 4.21** The setup of the in house respiratory motion phantom and ball cube for testing the targeting accuracy of the Synchrony respiratory tracking

c. The respiratory motion phantom switch was turned on and ensures that the phantom is centered to the imagers.

d. The LEDs markers were attached to the motion phantom. The markers were adjusted with a camera to check breathing pattern.

e. The correlation model was created. The x-ray image was acquired to match the plan DRRs. The technique of 110 kVp, 100 mA and exposure time of 50 ms was used. A short exported exposure time is always used.

f. The phantom was exposed with the moving various parameters to verify and study the correlation of amplitude of skin motion, respiratory rate and moving distance of tumor with the targeting accuracy of Synchrony<sup>®</sup> respiratory tracking system as shown in the table 4.1.

**Table 4.1** The Parameter's values for testing the synchrony<sup>®</sup> respiratory tracking

<b>Parameters</b>	<b>Amplitude (mm)</b>	<b>Respiratory rate (cycle/min)</b>	<b>Tumor motion (mm)</b>
<b>Amplitude (mm)</b>	6	15	25
	7.5	15	25
	9	15	25
	12	15	25
	15	15	25
<b>Respiratory rate (cycle/min)</b>	7.5	5	25
	7.5	10	25
	7.5	15	25
	7.5	20	25
	7.5	25	25
	7.5	30	25
<b>Tumor distance (mm)</b>	7.5	15	15
	7.5	15	25
	7.5	15	35

g. The exposed films were removed for analysis. Keep the films out of a UV light for 24 hours before being scanned.

#### 4.3.2.3 Film Analysis

a. The exposed and also unexposed films were scanned at the same time using a flatbed transparency scanner. During scanning, the anterior edge of the films is on the top and the left or superior edge is on the left of the image. Furthermore, these edges should not be varied more than 5 degrees from the actual image edges. However they should be as parallel as possible to the axes of the image.

b. The scanning images were loaded to End to End (E2E) Film Analysis 2.0 Software tool (Appendix D). All results of the centroid of dose distribution (total targeting error) were analyzed.

#### 4.3.2.4 Statistical analysis

All total targeting errors of the centroid of dose distribution for each parameter group were analyzed by using one way ANOVA (Analysis of Variance).

## CHAPTER V

### RESULTS

#### 5.1 Design and construction of the in-house respiratory motion phantom

The in-house respiratory motion phantom was constructed. As a result, the size of the motion phantom is  $17 \times 45 \times 15 \text{ cm}^3$  made of white acrylic plastic structure. The cam was driven by the gear motor 12 VDC. The phantom can be moved in two directions, supero-inferior with 15, 25 and 35 mm distances by tumor motion platform movement and antero-posterior in the range from 0 to 15 mm by moving the skin motion platform. By adjusting the voltage regulator, the respiratory rate can be varied from 0 to 30 cycles per minute. Figure 5.1 shows the construction parts of in-house respiratory motion phantom.



External structure  
(a)



Tumor motion platform  
(b)



Slash cut pipes  
(c)



Cam  
(d)

**Figure 5.1** Each part of in-house respiratory motion phantom (a) external structure (b) tumor motion platform (c) slash cut pipes (d) cam

Each part of in-house respiratory motion phantom was assembled. The switching power supply was connected to adjustable voltage regulator circuit and gear motor. Cam with 15, 25, or 35 mm slash cut pipes was attached to axle of gear motor. The skin motion platform is moved by cam and the tumor motion platform is pushed by slash cut pipe and pulls with tourniquet within the phantom. The completed in-house respiratory motion phantom was shown in figure 5.2

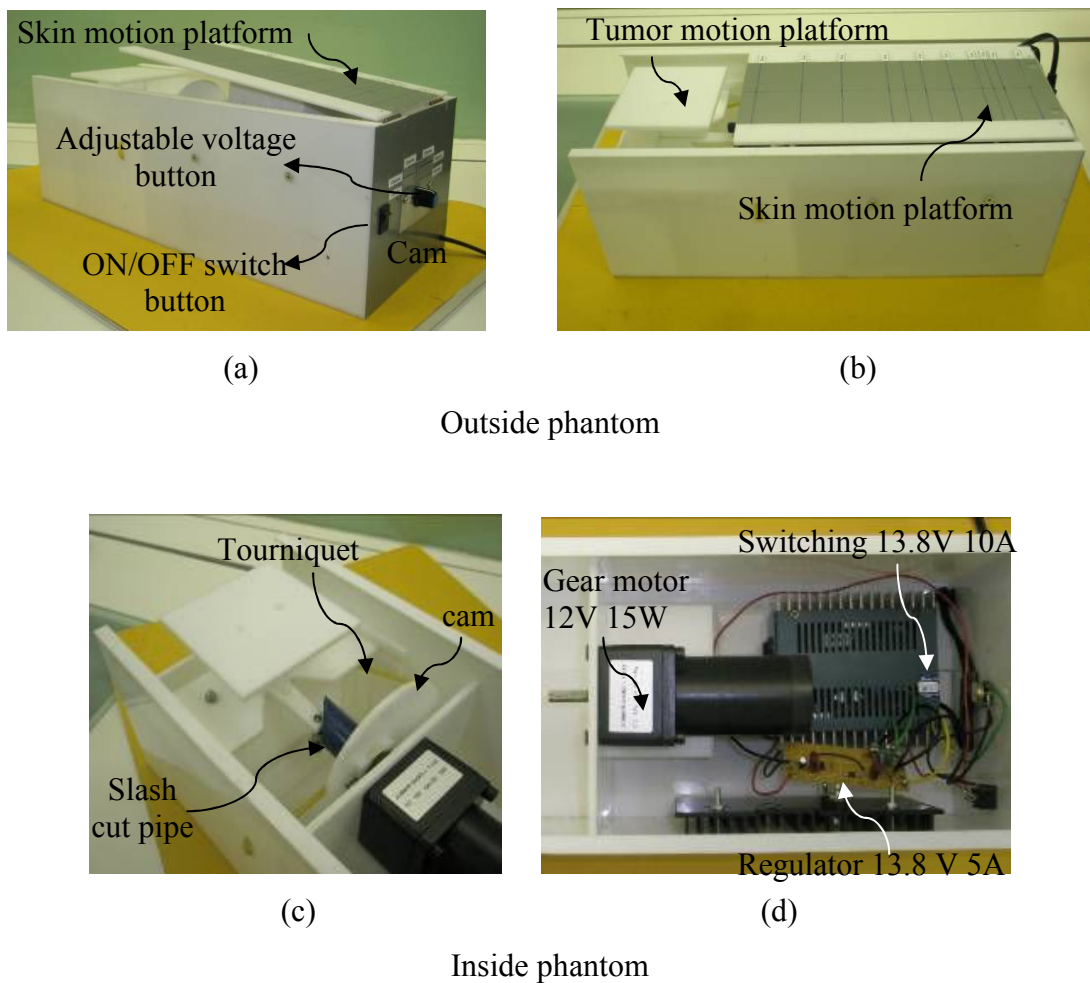


**Figure 5.2** The completed in-house respiratory motion phantom (a - b) outside phantom (c - d) inside phantom

## 5.2 Calibration and evaluation of the in-house respiratory motion phantom

The respiratory motion phantom was calibrated and evaluated by using the RPM (The Real-time Position Management™) system to define the amplitude positions of 6, 7.5, 9, 12, and 15 mm and respiratory rates of 5, 10, 15, 20, 25, and 30 cycles per minute.

For each amplitude and respiratory rate position, the calibration was repeated five times. Then each amplitude and respiratory rate position was marked on the motion phantom by using a permanent pen as shown in figure 5.3. Figure 5.4 shows the sinusoidal waves for the calibration of 7.5 mm amplitude position and respiratory rate of 15 cycles per minute (4 seconds per cycle).

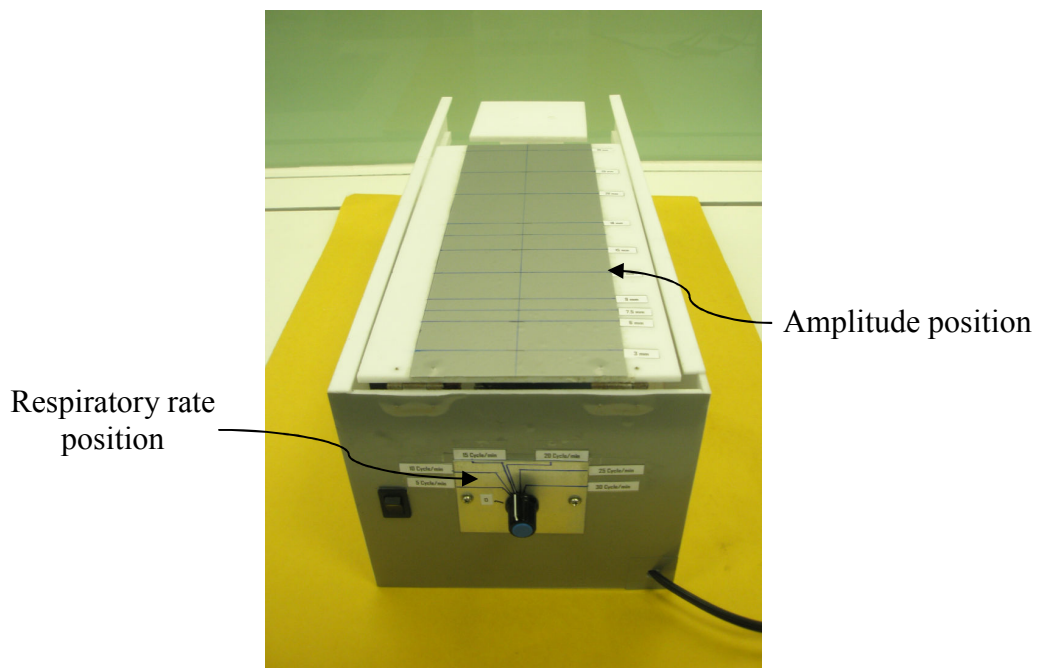


**Figure 5.3** The amplitude position (mm) on the skin motion platform and respiratory rate position of the respiratory motion phantom

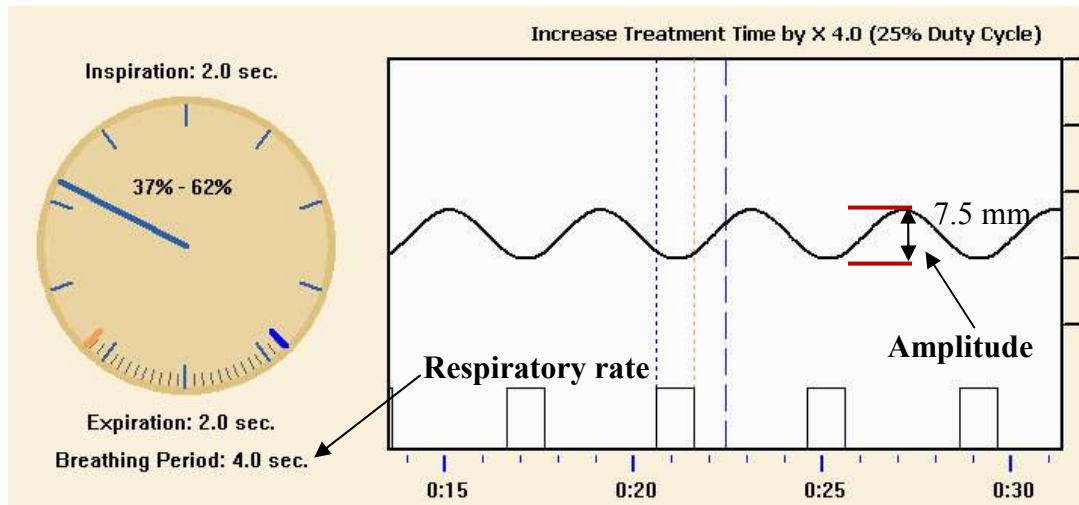


**Figure 5.4** Sinusoidal waves at amplitude position of 7.5 mm and respiratory rate of 15 cycles per minute (4 seconds per cycle) of the in-house respiratory motion phantom

Table 5.1 and 5.2 show the results of the precision test for amplitude position and respiratory rate, respectively.

**Table 5.1** The standard deviation of amplitude position (mm) of the in-house respiratory motion phantom

Setting value	Mean reading $\pm$ SD	Range (Min-Max)
6.0	6.0 $\pm$ 0	-
7.5	7.6 $\pm$ 0.22	7.5 - 8.0
9.0	9.0 $\pm$ 0	-
12.0	12.0 $\pm$ 0	-
15.0	15.0 $\pm$ 0	-

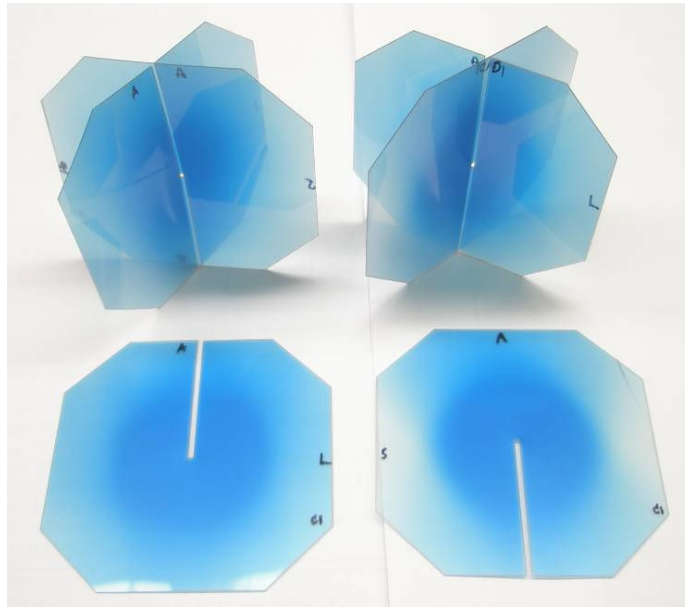
**Table 5.2** The standard deviation of respiratory rate (sec/cycle) of the in-house respiratory motion phantom

Setting value		Mean reading $\pm$ SD	Range (Min-Max)
Cycle/min	Sec/cycle		
5	12	11.98 $\pm$ 0.045	11.9-12
10	6.0	6.04 $\pm$ 0.089	6.0-6.2
15	4.0	4.0 $\pm$ 0.07	3.9-4.1
20	3.0	3.0 $\pm$ 0.0	-
25	2.4	2.4 $\pm$ 0.07	2.3-2.5
30	2.0	2.0 $\pm$ 0.0	-

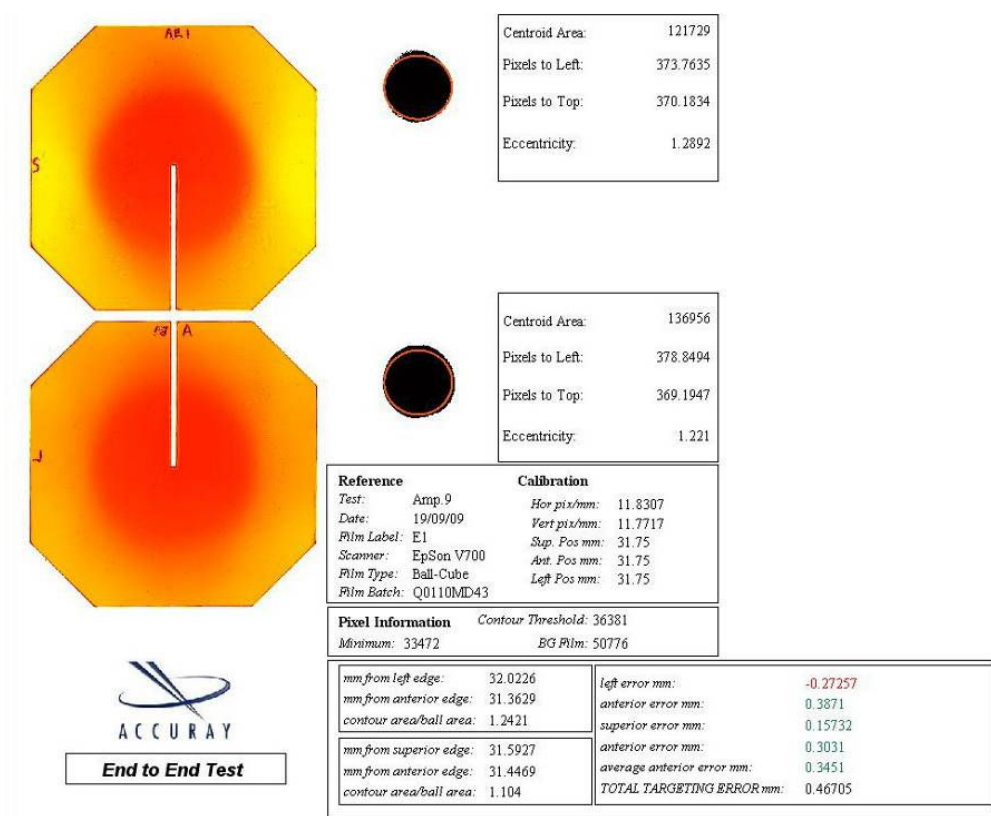
The maximum standard deviation measured of the amplitude of skin motion is 0.22 mm. Also the maximum standard deviation measured of the respiratory rate is 0.089 seconds per cycle.

### 5.3 Testing of the targeting accuracy of Synchrony<sup>®</sup> respiratory tracking system

From the film scanning, the errors of the target position in anterior, superior and left directions were obtained by using E2E software (appendix D). The total targeting errors (mm) were then calculated. Figure 5.5 shows (a) the exposed film and (b) digital centroid analysis with E2E software. The total targeting errors with various amplitudes of skin motion, respiratory rates and tumor motion distances are shown in table 5.3, 5.4, and 5.5, respectively.



(a)



(b)

**Figure 5.5** The example of (a) exposed films and (b) digital centroid analysis E2E software.

**Table 5.3** Total targeting errors (mm) of various amplitudes of skin motion for 15 cycles/min respiratory rate and 25 mm tumor motion distances

Amplitude	No.			Mean ± SD	
	1	2	3		
6	0.40	0.94	0.75	0.70	±0.27
7.5	0.31	0.65	0.34	0.43	±0.19
9	0.55	0.33	0.77	0.55	±0.22
12	0.45	0.63	0.57	0.55	±0.09
15	0.75	0.78	0.98	0.84	±0.13
<b>Mean ± SD</b>				<b>0.61</b>	<b>±0.22</b>

**Table 5.4** Total targeting errors (mm) of various respiratory rates for 7.5 mm amplitude of skin motion and 25 mm tumor motion distances

Respiratory rate (cycle/min)	No.			Mean ± SD	
	1	2	3		
5	0.53	0.37	0.61	0.50	±0.12
10	0.61	0.28	0.33	0.41	±0.18
15	0.31	0.65	0.34	0.43	±0.19
20	0.25	0.46	0.33	0.35	±0.11
25	0.79	0.32	0.583	0.56	±0.24
30	0.83	0.37	0.55	0.58	±0.23
<b>Mean ± SD</b>				<b>0.47</b>	<b>±0.18</b>

**Table 5.5** Total targeting errors (mm) of various tumor motion distances for 7.5 mm amplitude of skin motion and 15 cycles/min respiratory rate

Tumor distance (mm)	No.			Mean ± SD	
	1	2	3		
15	0.83	0.68	0.752	0.75	±0.08
25	0.31	0.65	0.34	0.43	±0.19
35	0.73	0.72	0.45	0.63	±0.16
<b>Mean ± SD</b>				<b>0.61</b>	<b>±0.19</b>

The mean values of the total targeting errors for the skin motion, respiratory rate and tumor motion distance are  $0.61 \pm 0.22$  mm,  $0.47 \pm 0.18$  mm, and  $0.61 \pm 0.19$  mm, respectively. By using the ANOVA statistical test to analyze the total targeting errors, there are no significant differences for the skin motion amplitudes from 6 to 15 mm (p-value = 0.1717, 95% CI), respiratory rate from 5 to 30 cycles/min (p-value = 0.5961, 95% CI) and tumor motion distance from 15 to 35 mm (p-value = 0.099, 95% CI).

## CHAPTER VI

### DISCUSSION

The in-house respiratory motion phantom was constructed and evaluated using the Varian RPM system. The phantom consists of two platforms for two directions of motion: superior to inferior with the distances of 15, 25, and 35 mm anterior to posterior from 0 to 15 mm. The respiratory rate can be varied from 0 to 30 cycles per minute. The measurement values in the standard deviation of amplitude of skin motion and respiratory rate indicated that the stability of the respiratory motion phantom is fairly stable and acceptable with maximum standard deviation of 0.22 mm amplitude and 0.089 seconds/cycle respiratory rate. This is due to stable voltage supplying to the gear motor. However, the problem of the respiratory motion phantom is the heat from the gear motor and the adjustable voltage regulator circuit which could be broken if it moves for a long period of time. This problem may be solved by moving the heat sink outside the phantom.

According to the evaluation of targeting accuracy of the Cyberknife with Synchrony<sup>®</sup> respiratory tracking system, although, the amplitude of skin motion, respiratory rate and tumor motion distance are varied in human standard range, the Synchrony<sup>®</sup> respiratory tracking system has sufficient performance for moving treatment target with the maximum error of  $0.61 \pm 0.22$  mm. The result agrees with the other studies, three Cyberknife centers [28] with the error of  $0.7 \pm 0.30$  mm and Wong et al [4, 29] with the error  $0.82 \pm 0.27$  mm. Consequently, the total system error of the Cyberknife system with Synchrony<sup>®</sup> respiratory tracking system could be ensured with error less than 1.0 mm which amplitude of skin motion, respiratory rate and tumor motion distance do not affect the targeting accuracy of Synchrony<sup>®</sup> respiratory tracking system. However, this system will be successful if respiratory training for patients is well performed. Nevertheless, the system will stop automatically when target is out of range from the correlation model which can cause several hours of treatment time.

In this study, the target deformation is beyond our scope. The Correlation model between the external marker and target positions motion is modeled just a simple linear relationship for this phantom. The nonlinear model for target deformation should be considered for future study.

## CHAPTER VII

### CONCLUSION

From this study, the in-house respiratory motion phantom was designed and constructed. The performance of the motion phantom was calibrated and evaluated using the Varian RPM system. The results show sufficient accuracy and stability with the precision better than 0.22 mm amplitude for skin motion and 0.089 seconds per cycle for respiratory rate. After evaluation, it was used to test the targeting accuracy of the Cyberknife system with the Synchrony<sup>®</sup> respiratory tracking system.

This motion phantom is very useful and convenient tool for independently testing the targeting accuracy of the Synchrony<sup>®</sup> respiratory tracking system.

The maximum targeting error of the Synchrony<sup>®</sup> respiratory tracking system tested by this respiratory motion phantom is  $0.61 \pm 0.22$  mm with skin motion test. By using ANOVA statistical test, it is found that the targeting accuracy of this system does not depend on amplitude of skin motion, respiratory rate and tumor motion distance (p-value > 0.099, 95% CI).

The testing of the Cyberknife with the Synchrony<sup>®</sup> respiratory tracking system using the respiratory motion phantom shows that it is suitable for clinical treatment with only a sub-millimeter error.

## REFERENCES

- 1 Kubo HD, Hill BC. Respiration gated radiotherapy treatment: a technical study. *Phys Med Biol* 1996; 41: 83-91.
- 2 Sharp GC, Jiang SB, Shimizu S, Shirato H. Prediction of respiratory tumour motion for real-time image-guided radiotherapy. *Phys Med Biol* 2004; 49: 425-40.
- 3 Chen QS, Weinhaus MS, Deibel FC, Ciezki JP, Macklis RM. Fluoroscopic study of tumor motion due to breathing: facilitating precise radiation therapy for lung cancer patients. *Med Phys* 2001; 28: 1850-6.
- 4 Wong KH, Dieterich S, Tang J, Cleary K. Quantitative measurement of CyberKnife robotic arm steering. *Technol Cancer Res Treat* 2007; 6: 589-94.
- 5 Sayeh S, Wang J, Main W, Kilby W, Maurer C. Respiratory Motion Tracking for Robotic Radiosurgery. *Treating Tumors that Move with Respiration* 2007 :15-29.
- 6 Keall PJ, Kini VR, Vedam SS, Mohan R. Motion adaptive x-ray therapy: a feasibility study. *Phys Med Biol* 2001; 46: 1-10.
- 7 Ozhasoglu C, Saw CB, Chen H, Burton S, Komanduri K, Yue NJ, et al. Synchrony--cyberknife respiratory compensation technology. *Med Dosim* 2008; 33: 117-23.
- 8 Vedam SS, Keall PJ, Kini VR, Mohan R. Determining parameters for respiration-gated radiotherapy. *Med Phys* 2001; 28: 2139-46.
- 9 Keall PJ, Mageras GS, Balter JM, Emery RS, Forster KM, Jiang SB, et al. The management of respiratory motion in radiation oncology report of AAPM Task Group 76. *Med Phys* 2006; 33: 3874-900.
- 10 Mageras GS, Pevsner A, Yorke ED, Rosenzweig KE, Ford EC, Hertanto A, et al. Measurement of lung tumor motion using respiration-correlated CT. *Int J Radiat Oncol Biol Phys* 2004; 60: 933-41.

- 11 Ozhasoglu C, Murphy MJ. Issues in respiratory motion compensation during external-beam radiotherapy. *Int J Radiat Oncol Biol Phys* 2002; 52: 1389-99.
- 12 Ahn S, Yi B, Suh Y, Kim J, Lee S, Shin S, et al. A feasibility study on the prediction of tumour location in the lung from skin motion. *Br J Radiol* 2004; 77: 588-96.
- 13 Benchetrit G. Breathing pattern in humans: diversity and individuality. *Respir Physiol* 2000; 122): 123-9.
- 14 Shirato H, Seppenwoolde Y, Kitamura K, Onimura R, Shimizu S. Intrafractional tumor motion: lung and liver. *Semin Radiat Oncol* 2004; 14: 10-8.
- 15 Dieterich S, Tang J, Rodgers J, Cleary K. Skin respiratory motion tracking for stereotactic radiosurgery using the Cyberknife.
- 16 Vedam SS, Kini VR, Keall PJ, Ramakrishnan V, Mostafavi H, Mohan R. Quantifying the predictability of diaphragm motion during respiration with a noninvasive external marker. *Med Phys* 2003; 30: 505-13.
- 17 Hoisak JD, Sixel KE, Tirona R, Cheung PC, Pignol JP. Correlation of lung tumor motion with external surrogate indicators of respiration. *Int J Radiat Oncol Biol Phys* 2004; 60: 1298-306.
- 18 Tsunashima Y, Sakae T, Shioyama Y, Kagei K, Terunuma T, Nohtomi A, et al. Correlation between the respiratory waveform measured using a respiratory sensor and 3D tumor motion in gated radiotherapy. *Int J Radiat Oncol Biol Phys* 2004; 60: 951-8.
- 19 Koch N, Liu HH, Starkschall G, Jacobson M, Forster K, Liao Z, et al. Evaluation of internal lung motion for respiratory-gated radiotherapy using MRI: Part I--correlating internal lung motion with skin fiducial motion. *Int J Radiat Oncol Biol Phys* 2004; 60: 1459-72.
- 20 Accury Physics Essentials guide 2006 Cyberknife System Manual (Synnyvale, CA: Accuracy (tm) Inc.).
- 21 Van Sornsens de Koste JR, Cuijpers JP, De Geest FG, Lagerwaard FJ, Slotman BJ, Senan S. Verifying 4D gated radiotherapy using time-integrated electronic portal imaging: a phantom and clinical study. *Radiat Oncol* 2007; 2: 32.

- 22 Respiratory gating platform. Standard imaging Inc.; Available from: [http://www.standardimaging.com/product\\_home.php?id=36](http://www.standardimaging.com/product_home.php?id=36).
- 23 Quasar<sup>TM</sup> Respiratory Motion Phantom. Modus Medical Devices Inc; Available from: [www.QUASARphantoms.com](http://www.QUASARphantoms.com).
- 24 Schweikard A, Shiomi H, Adler J. Respiration tracking in radiosurgery. *Med Phys* 2004; 31: 2738-41.
- 25 Murphy MJ. Tracking moving organs in real time. *Semin Radiat Oncol* 2004; 14: 91-100.
- 26 Murphy MJ. Image-guided motion adaption in radiotherapy. Arlington, VA, : Biomedical Imaging: From Nano to Macro, 2007. ISBI 2007. 4th IEEE International Symposium 12-15 April 2007.
- 27 Zhou T, Tang J, Dieterich S, Cleary K. A robotic 3-D motion simulator for enhanced accuracy in cyberknife stereotactic radiosurgery. *International congress series 12682004*: 323-8.
- 28 Dieterich S, Taylor D, Chang C. The Cyberknife Synchrony Respiratory Tracking System: Evaluation of systematic targeting uncertainty (White paper presented at ASTRO2004). Accuracy, Inc, Sunnyvale, CA, 2004.
- 29 Wong K, Dieterich S, Tang J, Wilson E, Cleary K. SU-FF-J-40: Independent Measurement of CyberKnife Synchrony Accuracy Using Optical Tracking. *Medical Physics* 2005; 32: 1928.
- 30 Kim G, Shim S, Chaung W, Min C, Kim J. The Evaluation of Tumor Motion and Treatment Accuracy in Liver Tumor using Synchrony Motion Tracking System (generation 4 Cyberknife). *Radiation Oncology Biology Physics* 2008; 72: S542.
- 31 King CR, Lehmann J, Adler JR, Hai J. CyberKnife radiotherapy for localized prostate cancer: rationale and technical feasibility. *Technol Cancer Res Treat* 2003; 2: 25-30.
- 32 Jang J, Kang Y, Choi B, Choi I, Kim M, Shin D, et al. Evaluation of the Accuracy of the CyberKnife. *World Congress on Medical Physics and Biomedical Engineering 2007*. : 2024-7.

- 33 Kuo JS, Yu C, Petrovich Z, Apuzzo ML. The CyberKnife stereotactic radiosurgery system: description, installation, and an initial evaluation of use and functionality. *Neurosurgery* 2008; 62: 785-9.
- 34 Antypas C, Pantelis E. Performance evaluation of a CyberKnife G4 image-guided robotic stereotactic radiosurgery system. *Phys Med Biol* 2008; 53: 4697-718.
- 35 Dieterich S, Pawlicki T. Cyberknife image-guided delivery and quality assurance. *Int J Radiat Oncol Biol Phys* 2008; 71: S126-30.
- 36 Adler JR, Jr., Murphy MJ, Chang SD, Hancock SL. Image-guided robotic radiosurgery. *Neurosurgery* 1999; 44: 1299-306; discussion 306-7.
- 37 Schweikard A, Glosser G, Bodduluri M, Murphy MJ, Adler JR. Robotic motion compensation for respiratory movement during radiosurgery. *Comput Aided Surg* 2000; 5: 263-77.
- 38 Murphy MJ, Cox RS. The accuracy of dose localization for an image-guided frameless radiosurgery system. *Med Phys* 1996; 23: 2043-9.
- 39 Muacevic A, Staehler M, Drexler C, Wowra B, Reiser M, Tonn JC. Technical description, phantom accuracy, and clinical feasibility for fiducial-free frameless real-time image-guided spinal radiosurgery. *J Neurosurg Spine* 2006; 5: 303-12.
- 40 Murphy MJ, Chang SD, Gibbs IC, Le QT, Hai J, Kim D, et al. Patterns of patient movement during frameless image-guided radiosurgery. *Int J Radiat Oncol Biol Phys* 2003; 55: 1400-8.
- 41 Chang SD, Main W, Martin DP, Gibbs IC, Heilbrun MP. An analysis of the accuracy of the CyberKnife: a robotic frameless stereotactic radiosurgical system. *Neurosurgery* 2003; 52: 140-6; discussion 6-7.
- 42 Romanelli P, Schaal DW, Adler JR. Image-guided radiosurgical ablation of intra- and extra-cranial lesions. *Technol Cancer Res Treat* 2006; 5: 421-8.
- 43 Seppenwoolde Y, Berbeco RI, Nishioka S, Shirato H, Heijmen B. Accuracy of tumor motion compensation algorithm from a robotic respiratory tracking system: a simulation study. *Med Phys* 2007; 34: 2774-84.

- 44 Lu XQ, Shanmugham LN, Mahadevan A, Nedeia E, Stevenson MA, Kaplan I, et al. Organ deformation and dose coverage in robotic respiratory-tracking radiotherapy. *Int J Radiat Oncol Biol Phys* 2008; 71: 281-9.
- 45 Nioutsikou E, Seppenwoolde Y, Symonds-Taylor JR, Heijmen B, Evans P, Webb S. Dosimetric investigation of lung tumor motion compensation with a robotic respiratory tracking system: an experimental study. *Med Phys* 2008; 35: 1232-40.
- 46 Synchrony respiratory tracking system 2008 (Accuracy Incorporated).
- 47 Stony Brook University Medical Center. Respiratory gating. 2007 [updated July 30,2009];Availablefrom:<http://stonybrookheartcenter.com/radiationoncology/respiratorygating>.
- 48 Hassan M. RPM Real-time Position (RPM Operationg Principles). Las Vegas,USA 2005 April 2005.
- 49 Accracy Inc. Cyberknife Traning. Sunnyvale,CA 2003 November 2003.
- 50 Sharma SC, Ott JT, Williams JB, Dickow D. Commissioning and acceptance testing of a CyberKnife linear accelerator. *J Appl Clin Med Phys* 2007; 8: 2473.

## **APPENDICES**

## APPENDIX A

### Cyberknife (Image guided robotic radiosurgery) system

The Cyberknife is a frameless robotic radiosurgery system that combines image guidance with robotic technology aiming at the delivery of highly conformal radiation dose distributions to target with standard uncertainty of less than 1 mm, invented by John Adler, who is a neurosurgeon at Stanford University. In August 2001, it was cleared by the Food and Drug Administration (FDA) for tumor treatment any anatomical site [27, 31-35]. This system consists of the treatment manipulator (robot), patient positioning system, the target locating system (TLS) and linear accelerator (Linac) which illustrated schematically in figure 1A [20, 33, 36-38].

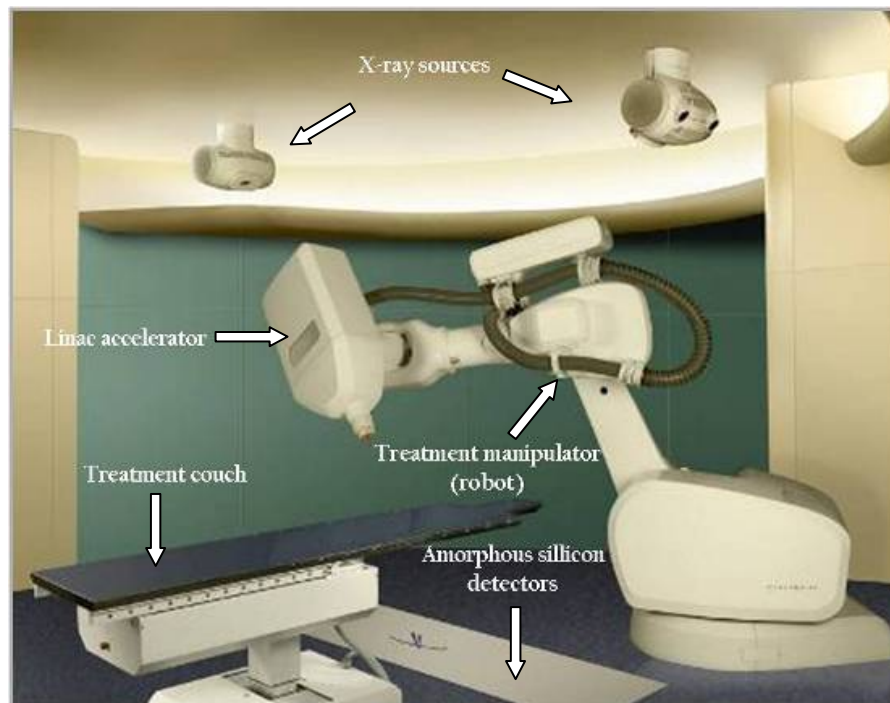


**Figure 1A** Main component of Cyberknife robotic radiosurgery system

The treatment manipulator (robot), a 6-axis manipulator is used for positioning and pointing the Linac to treatment target, provides a 65 -100 cm source to axis distance (SAD) with up to 1,200 treatment positions.

The patient positioning system includes the treatment couch. It is used to position the patient with automatic patient positioning technology which has motorized control of six degrees of freedom: three translations and three rotations.

The Target Locating System (TLS) has three components:

1. The x-ray sources are attached to the ceiling on each side of the treatment couch.
2. The x-ray generators supply high-voltage power to the x-ray source, 40-125 kV, 25-300 mA, 1-500 ms.
3. An amorphous silicon detectors are used along with the x-ray sources to correctly position the patient for treatment.

The linear accelerator is attached to the treatment manipulator and delivers radiation dose to the patient. It contains a compact 6 MV x-ray, dose rate 3, 4, and 6 Gy/minute, with 9.5 GHz X band accelerator. The secondary collimators are included in diameters of 5, 7.5, 10, 12, 15, 20, 25, 30, 35, 40, 50, and 60 mm.

In process, the target locating system is used to obtain the patient image during treatment. The acquired radiographs are automatically registered to digitally reconstructed radiographs (DRRs) derived from the treatment planning computed tomography (CT) for determining the patient's position. A control loop between the imaging system and the robotic arm allows the pointing of the treatment beam to be adapted automatically to the observed position of the treatment site. This allows the system to monitor and adjust to patient movement during treatment. The treatment beam can be directed at the treatment target [39, 40].

The advantages of the Cyberknife system include the ability to deliver treatment without a frame (frameless) which is noninvasive, increased fractionation flexibility, the ability to treat extra-cranial lesions and reduce the tumor motion margin in dose distribution while maintaining a 100% duty cycle for efficient dose delivery [31, 32, 41, 42].

## APPENDIX B

### Synchrony<sup>®</sup> respiratory tracking system

The Synchrony<sup>®</sup> respiratory tracking system (RTS) is subsystem of the Cyberknife treatment device to irradiate extra-cranial tumors that move due to respiration [43]. It is used to monitor patient breathing and adjust the radiation beam to match target organ, with goal of compensating for tumor motion due to respiration [27]. Within the treatment room, the Synchrony<sup>®</sup> camera array is mounted to the ceiling near the foot of the treatment couch and used for detecting the external LEDs marker [20]. With Synchrony, a correlation model between an internal organ motion (internal tumor position) and the skin respiratory motion (external marker position) is established by simultaneously taking x-ray images to track an internal fiducials and using infrared trackers (Synchrony<sup>®</sup> Tracking Marker LEDs) placed on the chest or abdomen. This correlation model is established and verified during treatment and also checked and updated regularly by acquisition of new pairs of x-ray image [44]. The linear accelerator follows the tumor motion based on the prediction from the external marker position and moves the linear accelerator dynamically with the target [11, 24, 27, 45]. This concept is illustrated in figure 1B



**Figure 1B** The Synchrony<sup>®</sup> Respiratory Tracking System

The main components of the Cyberknife with Synchrony<sup>®</sup> as shown in figure 2B are:

1. Linac with 6MV x-ray mounted to a robotic arm.
2. Two orthogonal flat-panel x-ray detectors positioned perpendicular to the x-ray source.
3. Synchrony<sup>®</sup> tracking vest is designed specifically for using with tracking markers, which are light-emitting diodes (LED).
4. Synchrony camera array holds 3 CCD (charge coupled device) cameras.
5. The Synchrony and the target locating system (TLS) computer

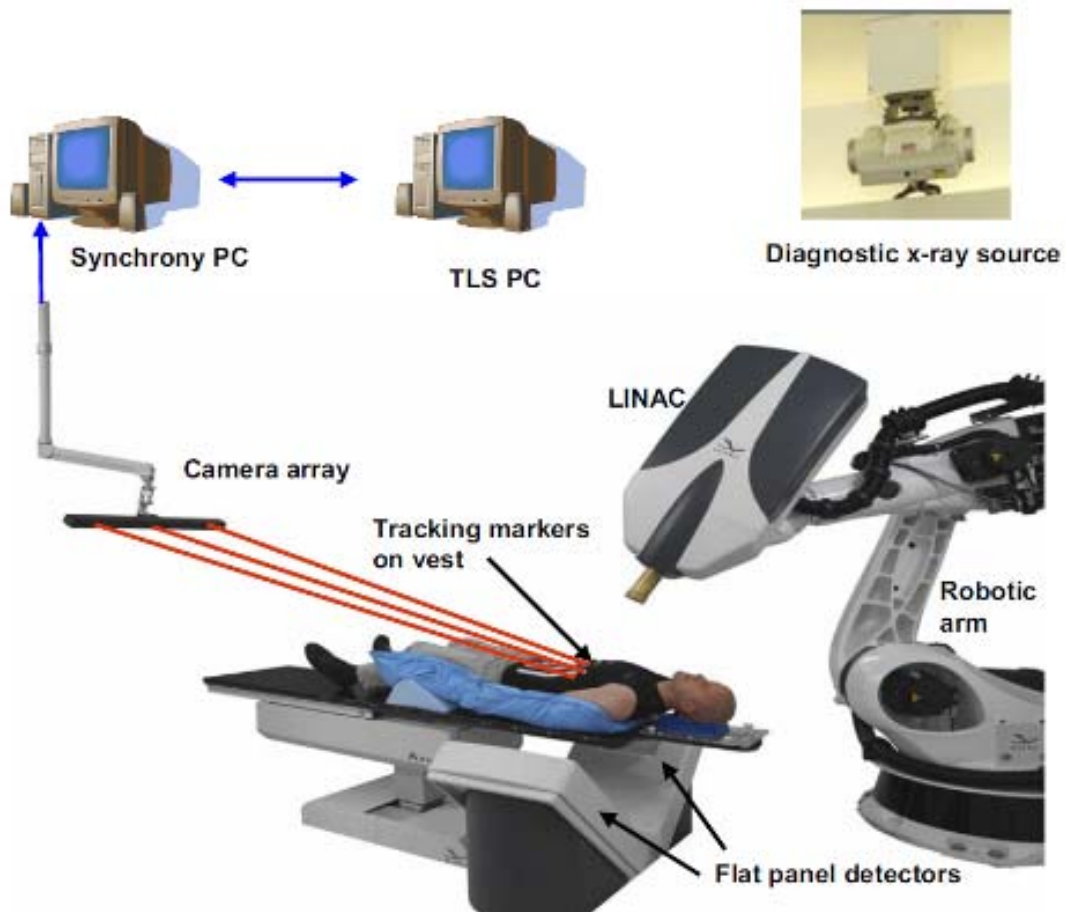


**Figure 2B** Main components of the Cyberknife robotic radiosurgery system with the Synchrony<sup>®</sup> respiratory tracking system

Step of working in Synchrony<sup>®</sup> respiratory tracking system are:

1. The target locating system (TLS) computer acquires x-ray image with a time stamp.
2. The Synchrony<sup>®</sup> computer uses the time stamp to identify the location of the internal tumor markers.
3. The Synchrony<sup>®</sup> computer sent the calculated target location to the TLS computer at that time stamp.
4. The TLS computer extracts and identifies the internal tumor marker in the live image. The actual target location is sent to the Synchrony<sup>®</sup> computer with the time stamp.
5. The Synchrony<sup>®</sup> computer checks the agreement of the actual target location and the calculated target location is less than 5 mm. If not, an ESTOP is initiated which the treatment is paused.
6. A robot moves on to the next beam delivery location within 2-3 s.

The correlation model between internal tumor and external marker position is generated by fitting the 3D internal tumor position at respiratory cycle to the simultaneous external marker position. The tumor position is determined by detecting fiducial or internal tumor markers in x-ray images. The tumor position and the time at which the image was acquired are sent to the Synchrony computer. The continuously measured external marker positions are stored in a buffer. The image acquisition time is used to find the corresponding position and velocity of all the markers. For each marker, a data point consisting of the marker position, marker velocity, and target position is added to its data set. As each new data point is added, the parameters for each correlation model type are computed.

For the Synchrony<sup>®</sup> system process, prior to treatment, a 2-4 small gold fiducial markers embedded at the tumor site. After approximately 1 week, a patient returned for planning CT. The patient lay comfortably supine and wore a Synchrony tracking vest. The vest was form-fitting and highly elastic to ensure that it moved with the patient's chest wall or abdomen as illustrated in figure 3B



**Figure 3B** Three LED markers are attached to vest that the patient wears during treatment

On the day of treatment, the patient was wore a Synchrony tracking vest and lay supine on the treatment couch in the same immobilization device that was used during the planning CT scan. The 3 LED markers (External markers) were attached to the patient's chest or abdomen. The camera array continuously registered the positions of external markers and reported them to the Synchrony<sup>®</sup> computer. The x-ray imaging is synchronized with optical tracking of external markers [7]. During the initialization stage of the procedure, a correlation model is computed, using least-squares fit of all available data points. Then the linear, single, and dual quadratic models are considered [5].

Each model provides an estimate of the internal tumor position from the external marker position:

$$\mathbf{X}_{Ti} = f_i(\mathbf{X}_{Mi}) \quad (1)$$

Where  $\mathbf{X}_{Mi}$  is the position vector of the  $i$ th marker.

$\mathbf{X}_{Ti}$  is the position vector of the target estimated from the  $i$ th marker.

When more than one internal tumor marker, the average value of the individual tumor position is used estimate of the target position.

Even if the external marker and internal tumor position follow linear trajectories the linear model is built. Using this simplification, the correlation model can be written as:

$$\mathbf{X}_{Ti} = f_i(r_i) \tag{2}$$

Where  $r_i$  represents the distance traveled along each marker's principal axis of motion.

The initial release of the Synchrony<sup>®</sup> system used only a linear function for  $f_i$ :

$$\mathbf{X}_{Ti} = \mathbf{A}r_i + \mathbf{B} \tag{3}$$

The linear coefficients  $\mathbf{A}$  and  $\mathbf{B}$  are vector-valued quantities. The linear correlation model is easy to build and robust which it provides accurate tracking results for many patients.

Even if the external marker and internal tumor position separate the trajectories during inhalation and exhalation (hysteresis or phase difference), the correlation between the external marker and tumor positions will be nonlinear, the nonlinear models (single and dual quadratic models) are built.

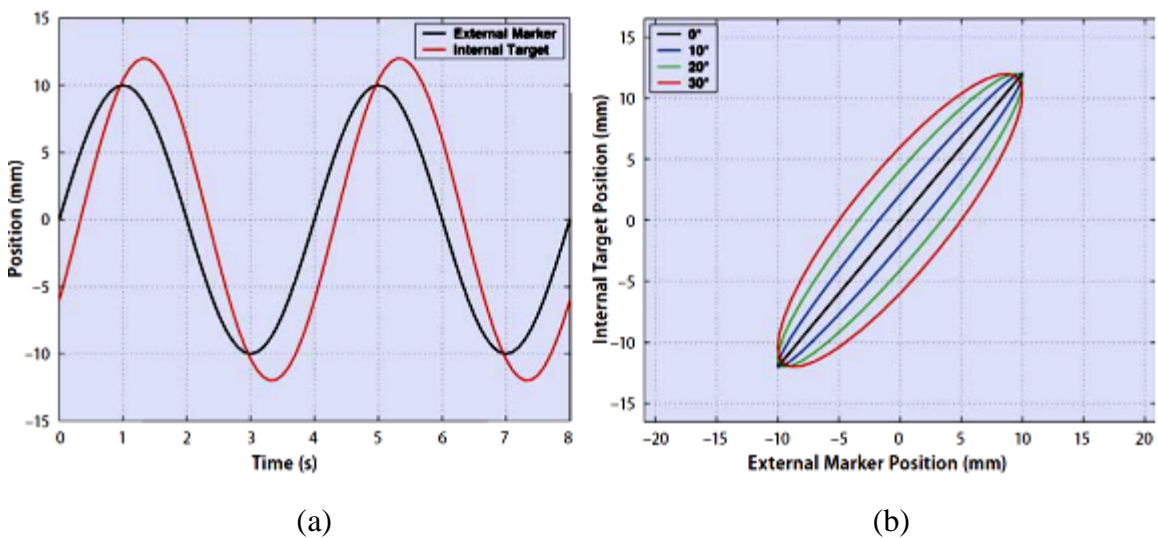


**Figure 4B** Illustration of (a) phase difference and (b) its effect on correlation between external marker and target positions [5].

A dual-curvilinear two polynomials model was used to separately model the inhalation and exhalation phases of the respiratory cycle:

$$X_{TI} = \begin{cases} \sum_{j=0}^N A_j^+ r_i^j & \dot{r} \geq -\dot{r}_{min} \\ \sum_{j=0}^N A_j^- r_i^j & \dot{r} \leq \dot{r}_{min} \end{cases} \quad (4)$$

Where  $\dot{r}$  represents the external marker velocity

$r_i^j$  represents the distance traveled along each marker's principal axis of motion

$N = 1$ , which is the linear model in Eq. (3), and  $N = 2$ , which is a quadratic model.

A dual quadratic model, if the external marker position is outside of the range of the linear correlation model, a quadratic fit is considered [5].

After the correlation model is built, it can be used to predict the tumor position based on the position of external optical markers. The predicted position computed from the model can be compared to the actual position of the tumor extracted from the real-time x-ray images. The discrepancy between the predicted position and the actual position is reported in real time by Synchrony<sup>®</sup> tracking software. If the discrepancy is greater than 5 mm, the radiation beam is turned off automatically and a new correlation model can be rebuilt [5, 7, 24, 37].

Advantages of The Synchrony<sup>®</sup> respiratory tracking system are that patients can breathe normally that there is no loss of Linac duty cycle such as with gate therapy, the localization of the internal tumor position is very precise and does not depend on patient position error and minimized irradiation of normal tissue or critical structures [43, 46].

## APPENDIX C

### **Real-time Position Management<sup>TM</sup> (RPM) System**

The Varian® Real-time Position Management<sup>TM</sup> (RPM) system is video based system that tracks a patient's respiratory cycle to correlate tumor position. Using an infrared tracking CCD (Charge coupled device) camera and a reflective marker block, the system measures the patient's respiratory pattern and period of motion in waveform. The gating thresholds are set when the tumor is in the desired portion of the respiratory cycle. These thresholds determine when the gating system turns the treatment beam on and off [47].

The system uses video tracking of marker block with CCD video camera and infrared illuminator. The CCD camera is fixed to the wall of treatment room or to the CT couch in the CT simulation room and images in real-time a lightweight plastic block with reflective markers attached to it. The marker block is placed on the patient chest or abdomen. The reflective markers on the plastic block that reflect the infrared (IR) coming from the illuminator mostly back towards the IR light source. Each video camera frame is digitized in real-time which is analyzed by real-time tracking software. For each image are detected the presence and locates the centroid of the two markers on the block in pixel coordinate. When marker block is move, the real-time position signal, the respiratory signal period, amplitude and phase is showed control panel [48].

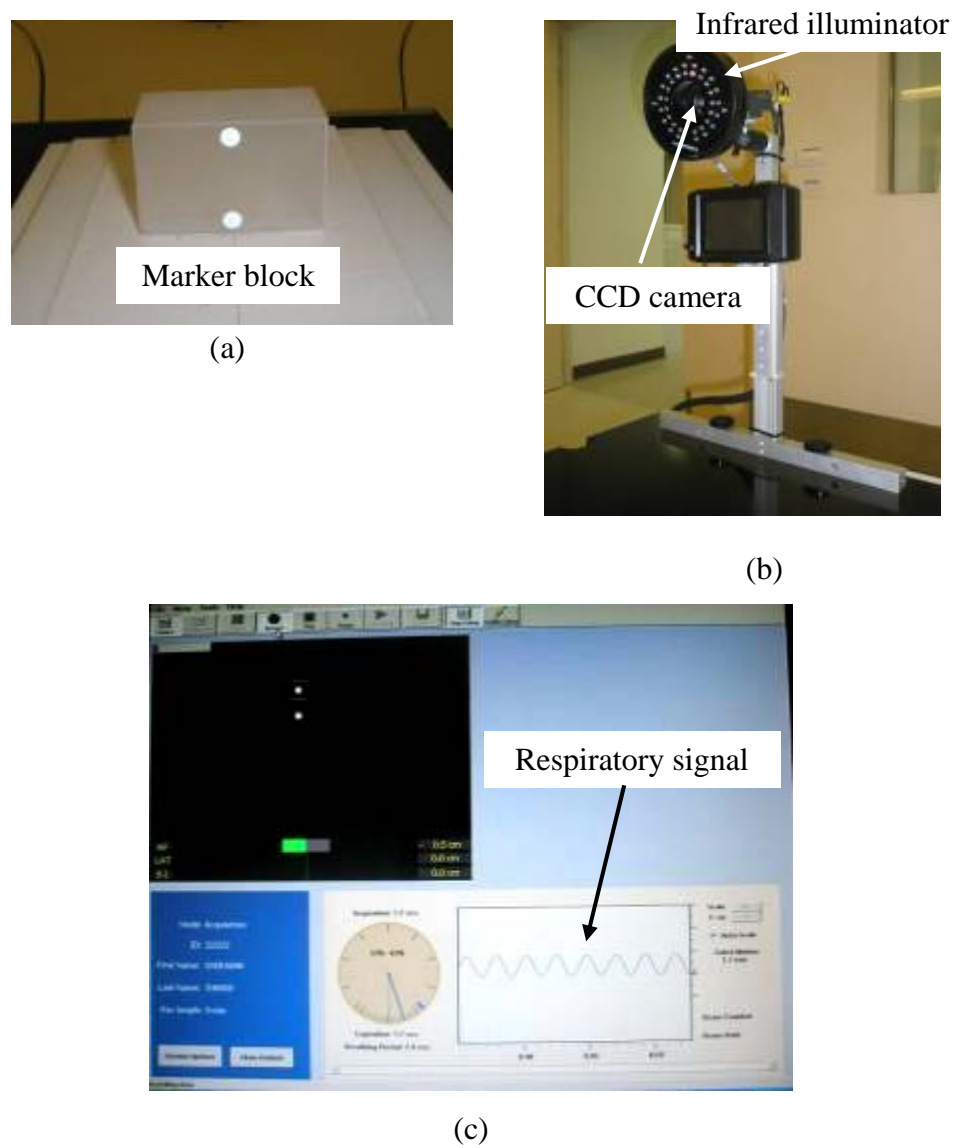


**Figure 1C** The Real-time Position Management™ (RPM) System. (a) The marker block with two reflective markers. (b) CCD camera and infrared illuminator (c) the real-time position signal is showed control panel.

## APPENDIX D

### The E2E test (End to end test)

The E2E test is designed to test the overall geometric targeting accuracy of the Cyberknife system. The ball-cube dose distribution recorded on film reflects the targeting accuracy based on radiation delivered to the ball-cube phantom.

The ball-cube phantom (Figure 1D) was used for testing the targeting accuracy of Synchrony<sup>®</sup> respiratory tracking system. Orthogonal radiochromic films can be placed within the 4 pieces ball-cube phantom which connects together using threaded nylon rods and nuts. A 31.75 mm diameter acrylic ball is placed in the center of cube. For application, a ball-cube with 2 pieces of film was loaded into the ball phantom for testing the targeting accuracy.

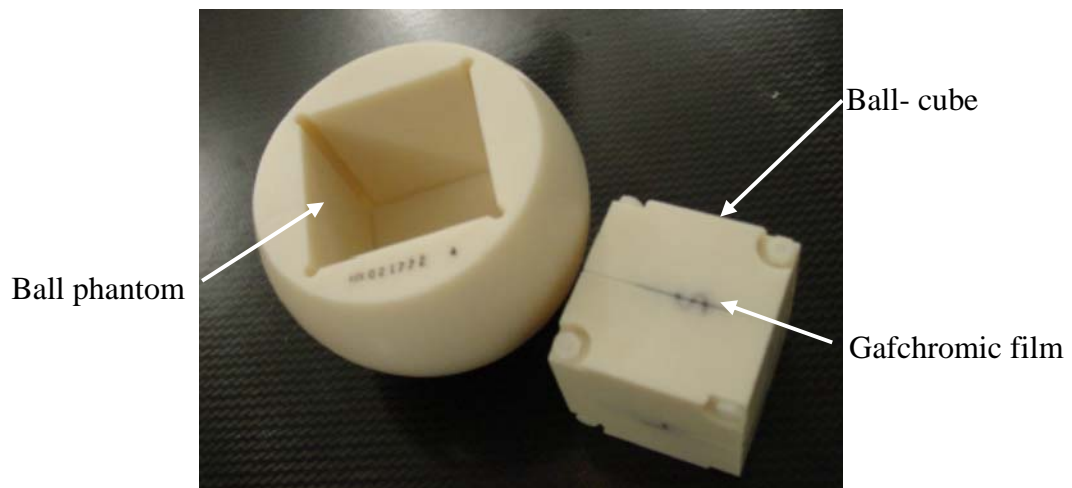


**Figure 1D** The ball-cube phantom

In process of E2E test, a treatment plan is generated with the goal of conforming the isodose line to the target ball (for this research, 80% contour aiming at 31.75 mm target ball). After the delivery, a two exposed films and unexposed film are scanned and analyzed using film analysis software package of Accuray. The software

calculates the distance between the centers of the planned and delivered dose distributions. These results indicate the accuracy and stability of the system's non-isocentric beam geometry. Radiochromic film is suitable for this process because of its relative insensitivity to ambient light and also because of the relatively high dose characteristics of radiosurgery procedures [32, 49, 50].

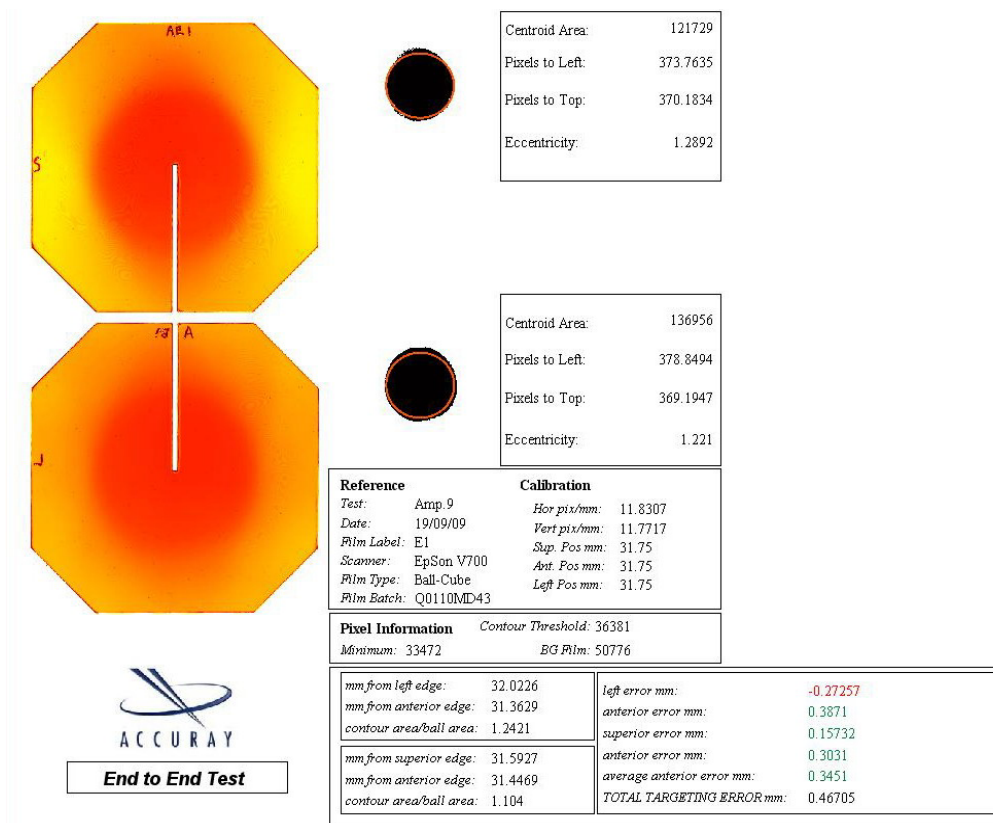


Figure 2D Analysis software package provided by Accuray for E2E test

## **BIOGRAPHY**

<b>NAME</b>	Mr.Chirasak Khamfongkhrua
<b>DATE OF BIRTH</b>	2 August 1984
<b>PLACE OF BIRTH</b>	Sukhothai, Thailand
<b>INSTITUTIONS ATTENDED</b>	Naresuan University, 2007: Bachelor of Science (Radiological Technology) Mahidol University, 2010: Master of Science (Medical Physics)
<b>RESEARCH GRANTS</b>	-
<b>HOME ADDRESS</b>	60/1 Moo 10, Khoakaeosisombun, Thungsaliang, Sukhothai, Thailand 64230
<b>POSITION&amp;OFFICE</b>	54 Chulabhorn Hospital, Bangkok, Thailand 10210 Position: Medical Physicist Tel. 0-2576-6040
<b>PUBLICATION/PRESENTATION</b>	- The 47 <sup>th</sup> Annual Scientific Meeting of Royal College of Radiologist & Radiological Society of Thailand and The 4 <sup>th</sup> Annual Meeting Thai Medical Physicist Society (25 March 2010) - Journal of Thai Society of Therapeutic Radiology and Oncology, Volume 16, No.2 July – December 2010